

# SPS impedance modeling

C. Zannini, G. Rumolo, B. Salvant, V.G. Vaccaro

Acknowledgments: T. Argyropoulos, M. Barnes, N. Biancacci,  
J. Bauche, S. Bouleghlimat, F. Caspers, H.A. Day, G. De  
Michele, E. Metral, N. Mounet, Y. Sillanoli, M. Taborelli, M.  
Van Stenis, V.G. Vaccaro

# Overview

- Updated status of the SPS impedance model

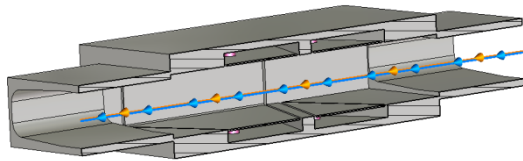
## Improvement of the model

- Kicker impedance model
  - Improvement of the model
    - C-Magnet model
    - Realistic models
    - Comparisons with bench impedance measurements
- Resistive wall impedance
  - A more realistic model

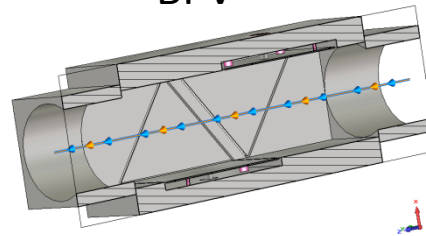
# Updated status of the SPS impedance model

- Elements included in the database:
  - Realistic model that takes into account the different SPS vacuum chambers weighted by the respective length and beta function. Also the iron in the magnet is taken into account
  - 19 kickers (CST 3D simulation)
  - 106 BPHs (CST 3D simulations)
  - 96 BPVs (CST 3D simulations)
  - 200 MHz cavities without couplers (CST 3D simulations)
  - 800 MHz cavities without couplers (CST 3D simulations)
  - Enamel flanges

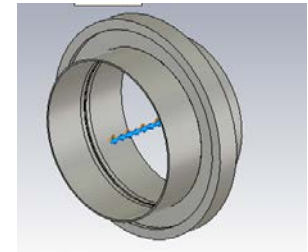
BPH



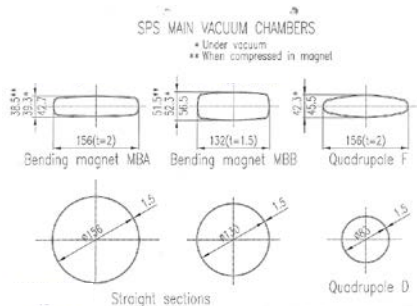
BPV



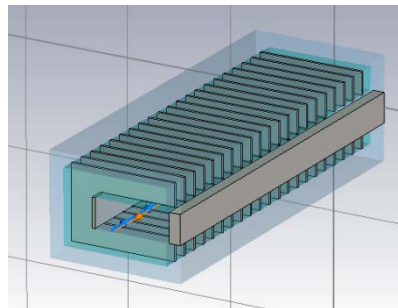
Enamel flanges



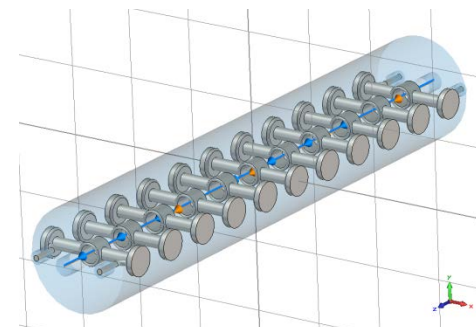
Beam pipe



Kickers



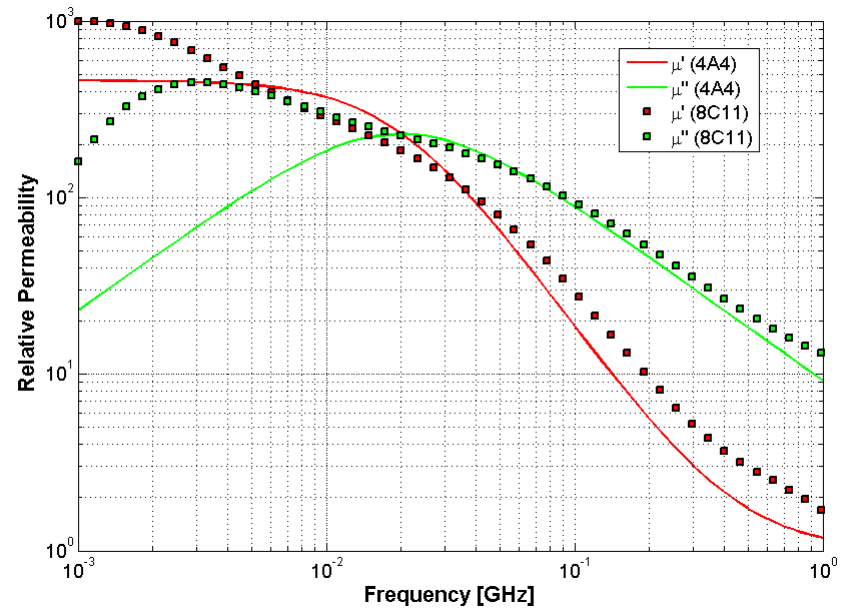
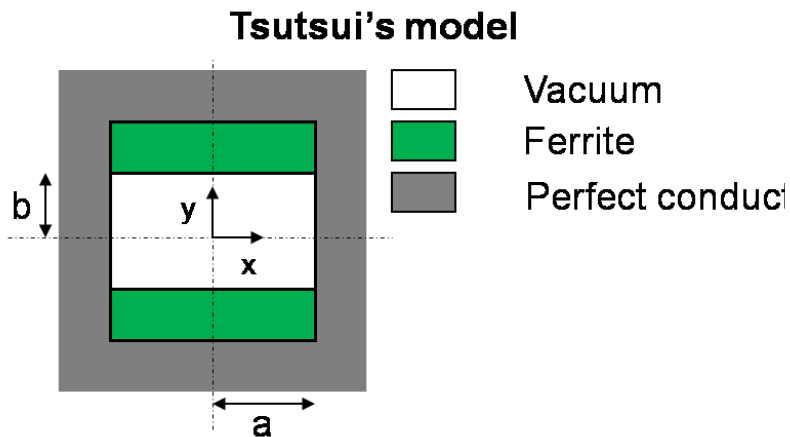
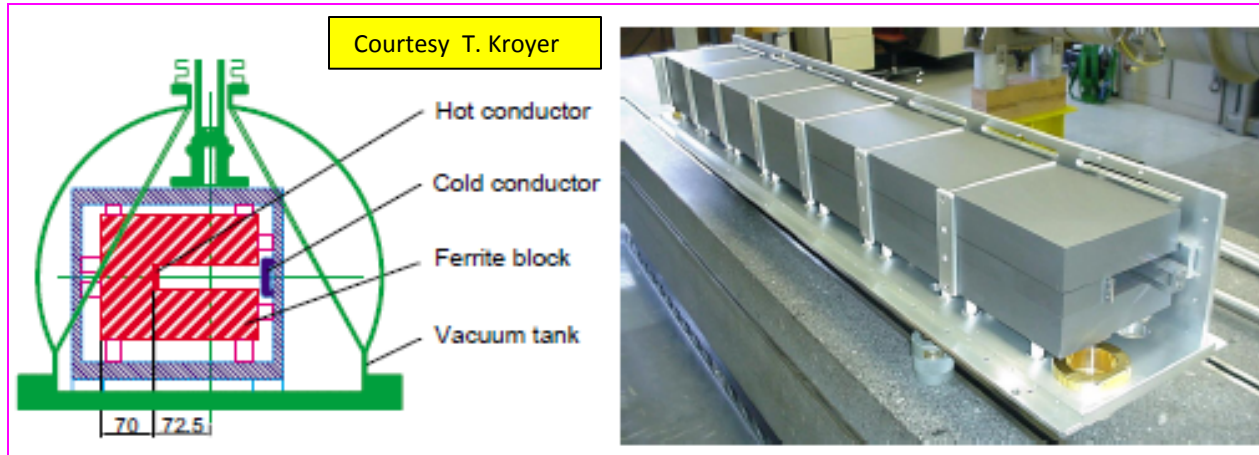
TW 200MHz and 800MHz



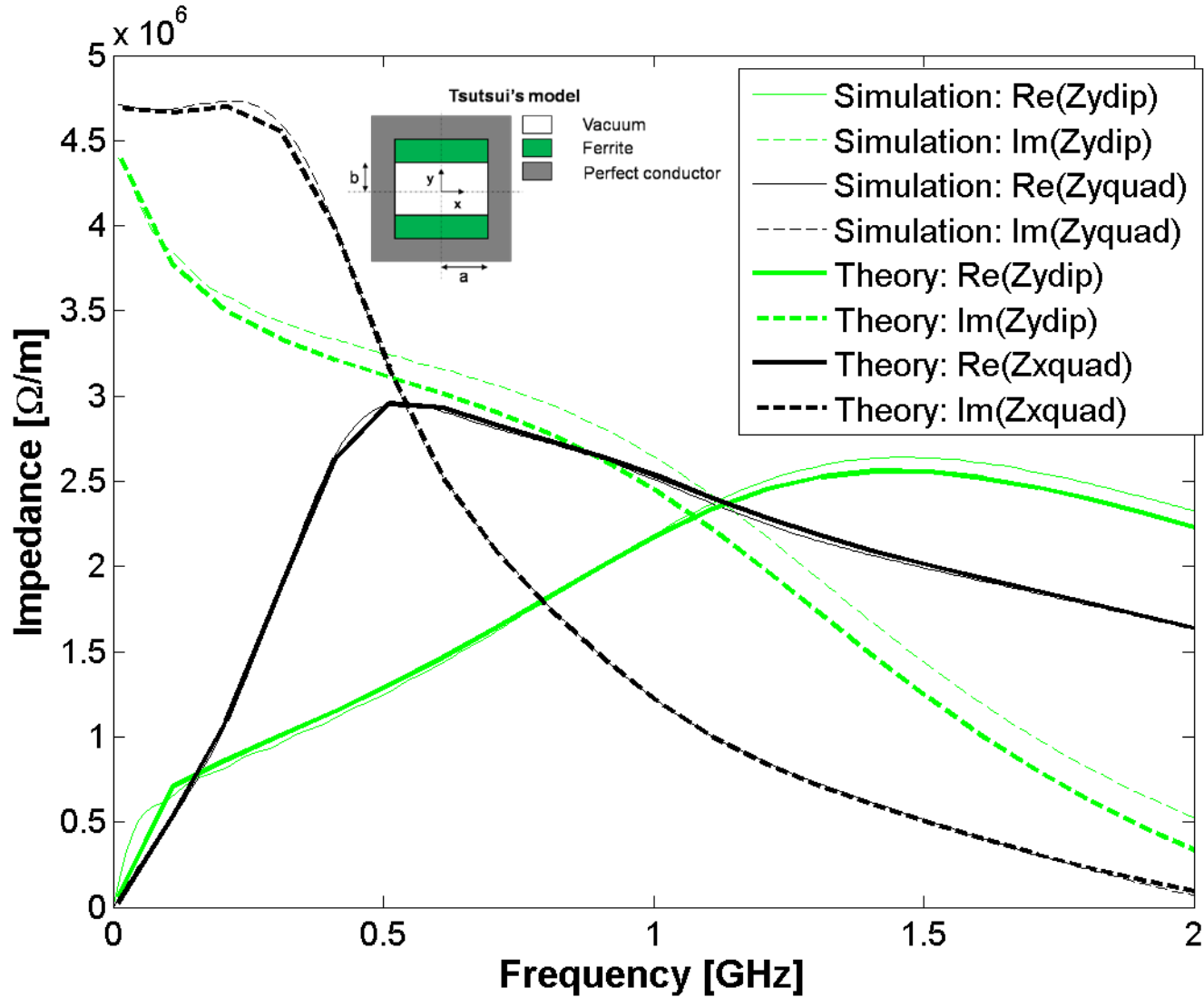
# Overview

- Updated status of the SPS impedance model
- Improvement of the model
  - Kicker impedance model
    - Status of the SPS kicker impedance model
    - Improvement of the model
      - C-Magnet model
      - Realistic models
      - Comparisons with bench impedance measurements
  - Resistive wall impedance
    - Status of the SPS wall impedance model
    - A more realistic model

# Simplified kicker model

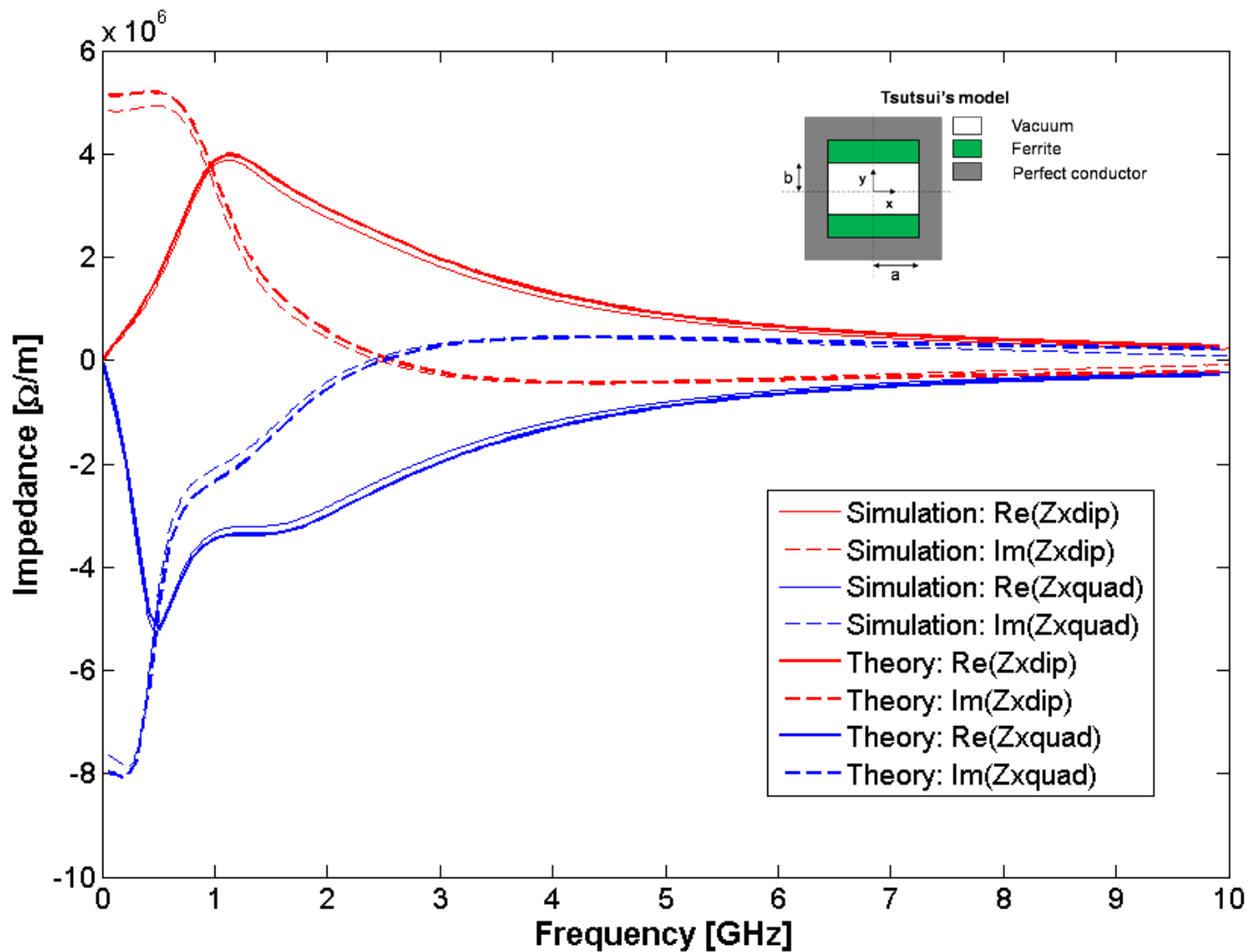


# Vertical impedances for all the SPS kickers



The theoretical predictions and simulations are in very good agreement

# Horizontal impedance from all the SPS kickers



The theoretical predictions and simulations are in very good agreement

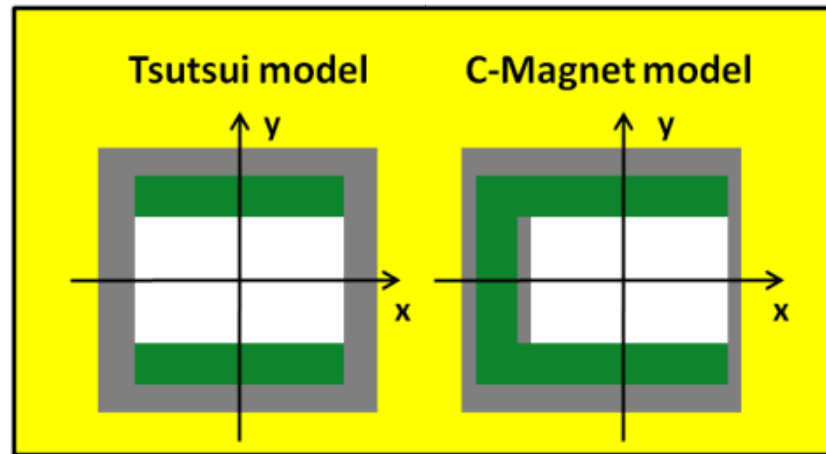
We are confident with the 3D TD EM simulation code (CST Particle studio)

# Overview

- Updated Status of the SPS impedance model
- Improvement of the model
  - Kicker impedance model
    - Status of the SPS kicker impedance model
    - Improvement of the model
      - C-Magnet model
      - Realistic models
      - Comparisons with bench impedance measurements
  - Resistive wall impedance
    - Status of the SPS wall impedance model
    - A more realistic model



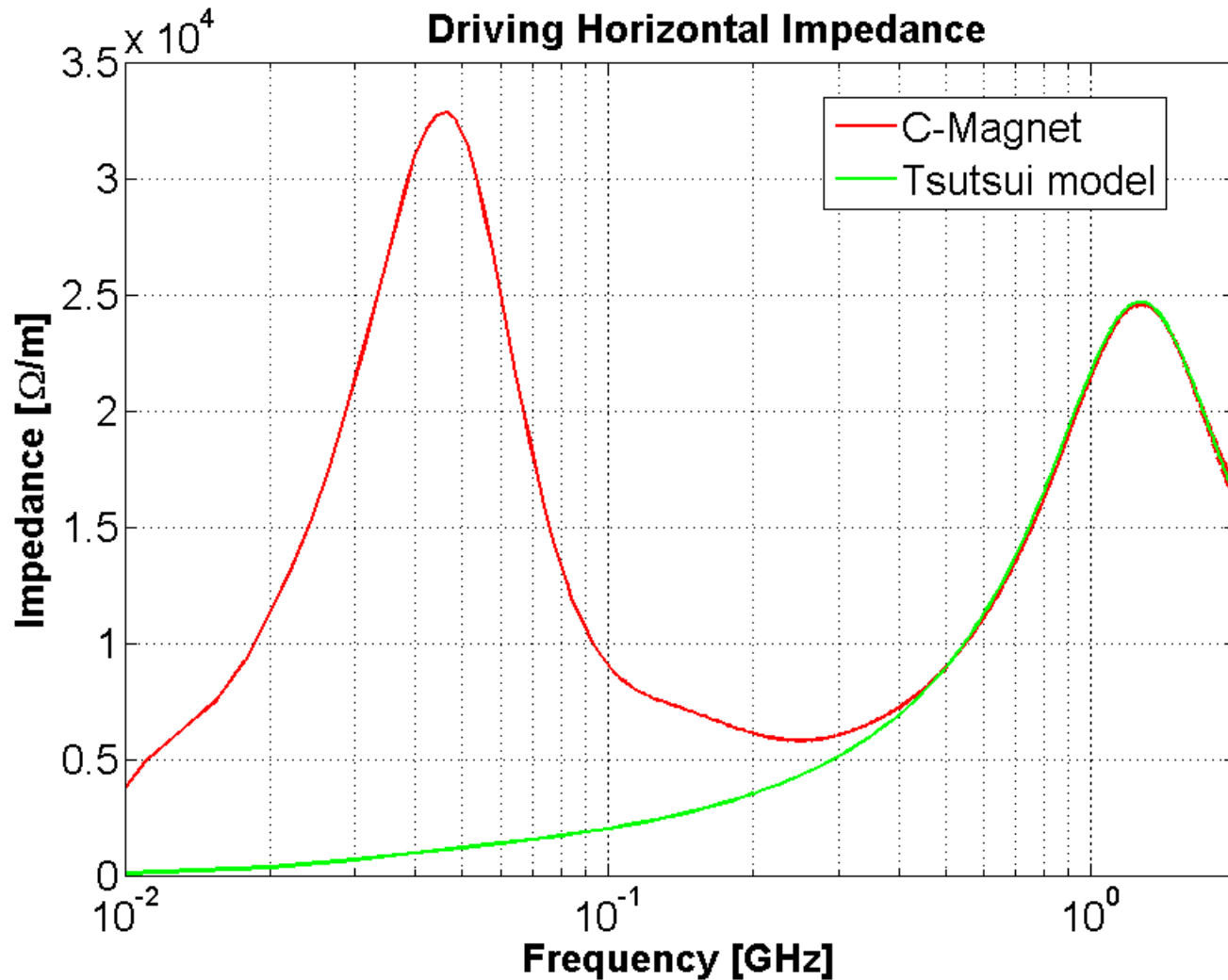
# Improving the model



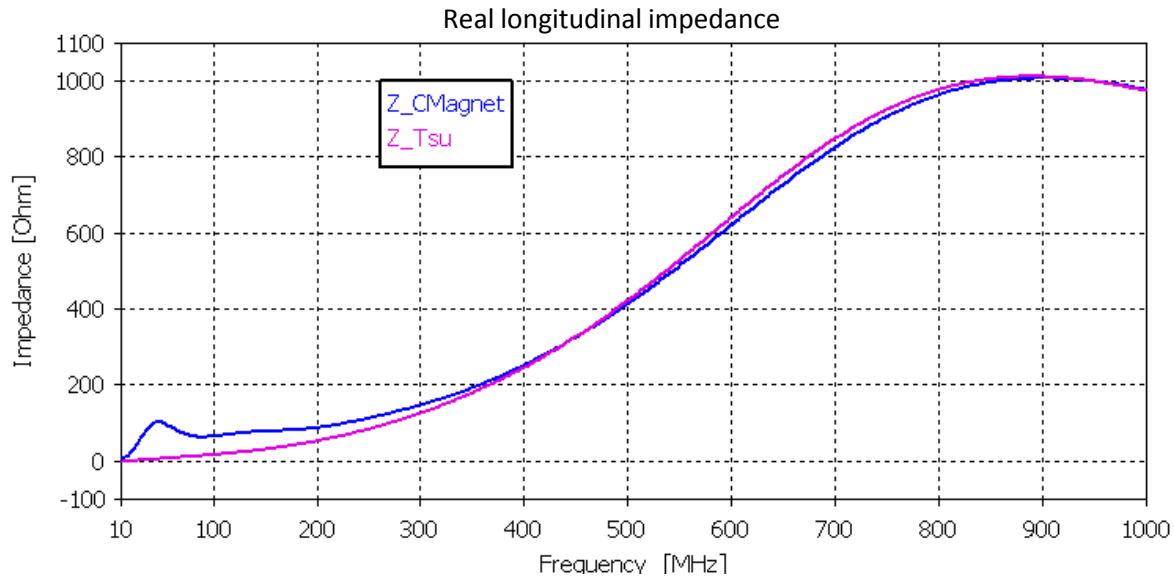
In the real structure there is a TEM propagation (finite length effect)

The TEM mode plays a role when the penetration depth in the ferrite becomes comparable to the magnetic circuit length (below few hundred MHz).

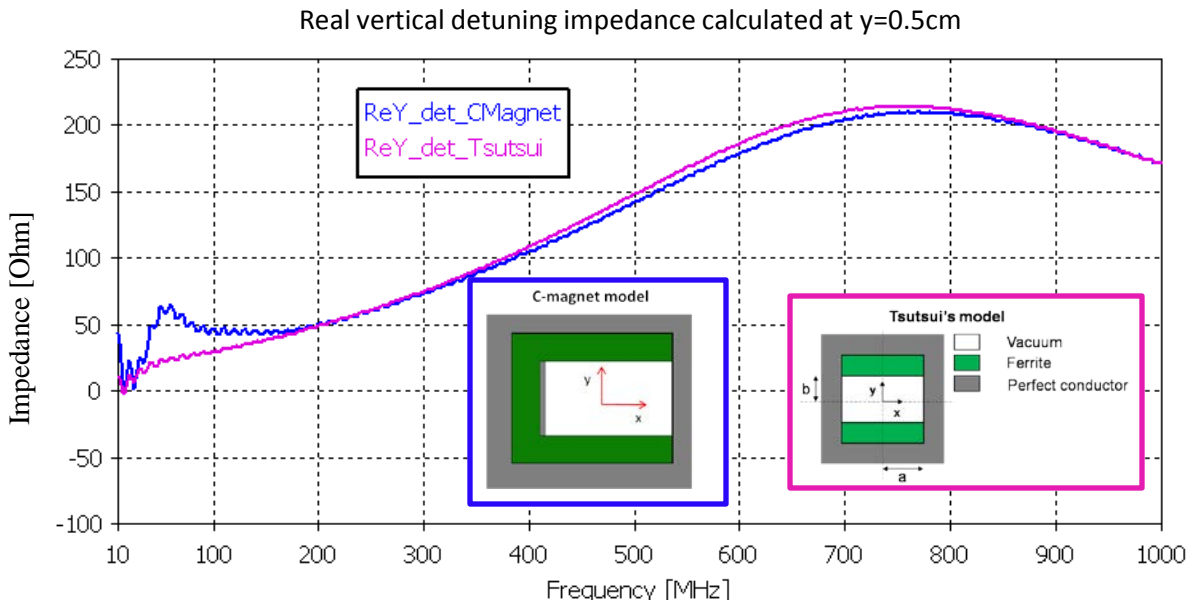
# C-magnet: driving horizontal impedance



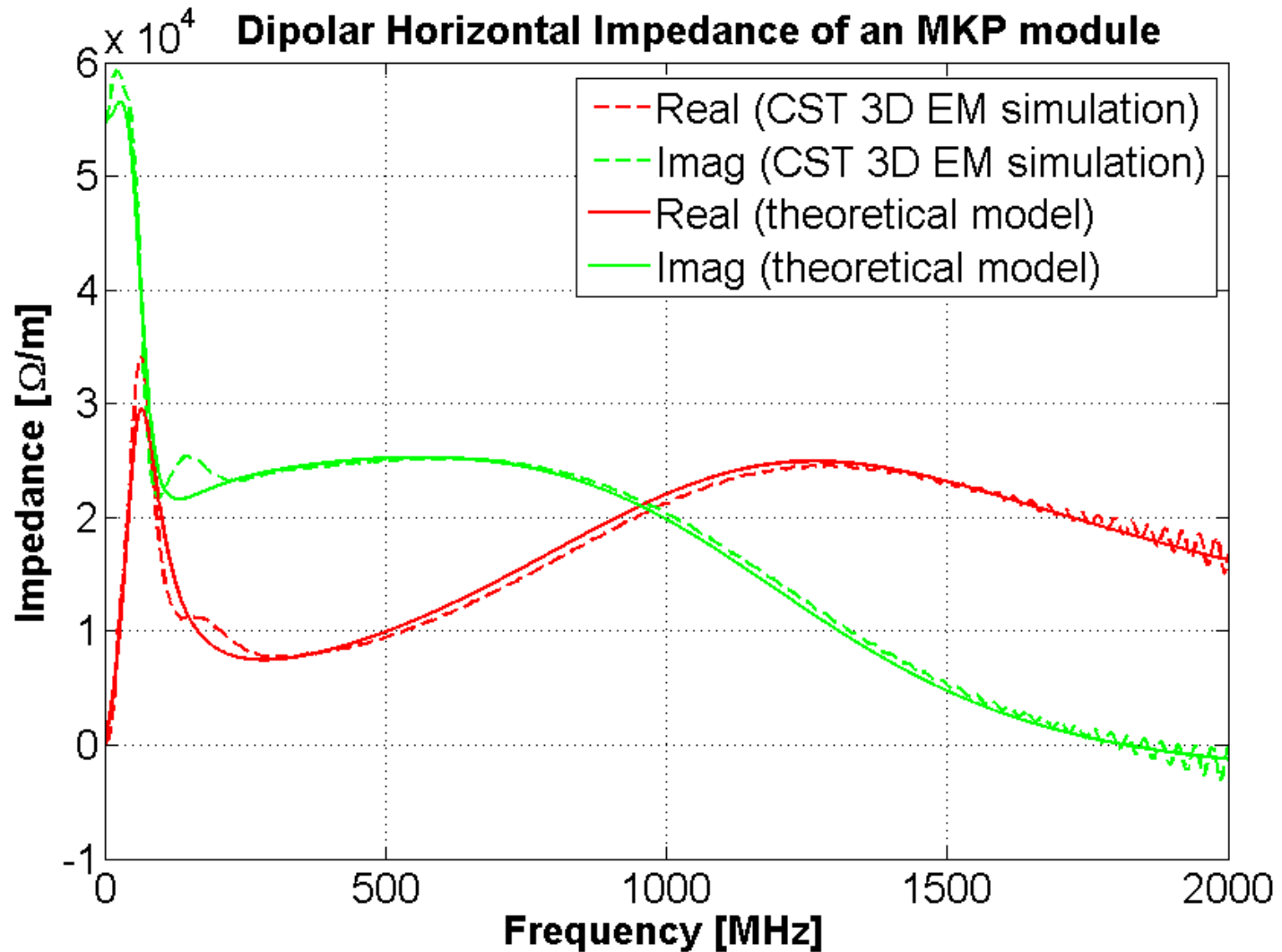
# Comparing the two models



We can see the peak also in the longitudinal and vertical impedance



# C-Magnet: 3D theoretical model for impedance calculation

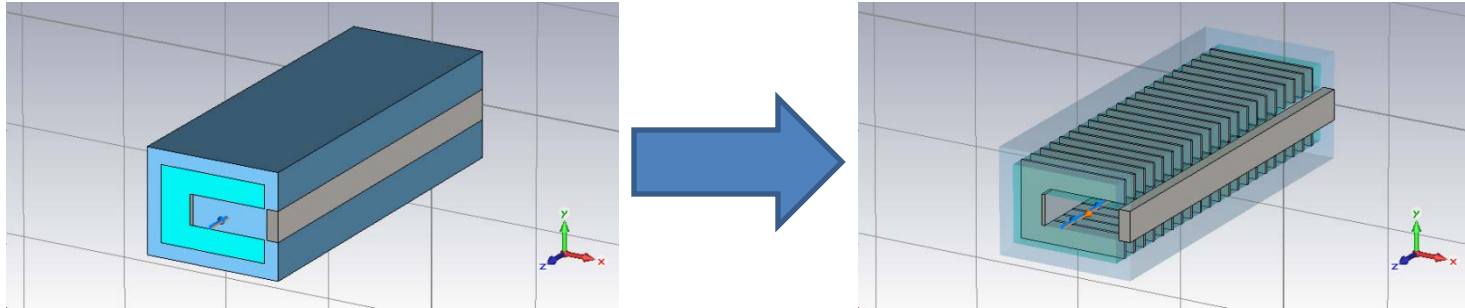


The theoretical predictions and simulations show a very good agreement

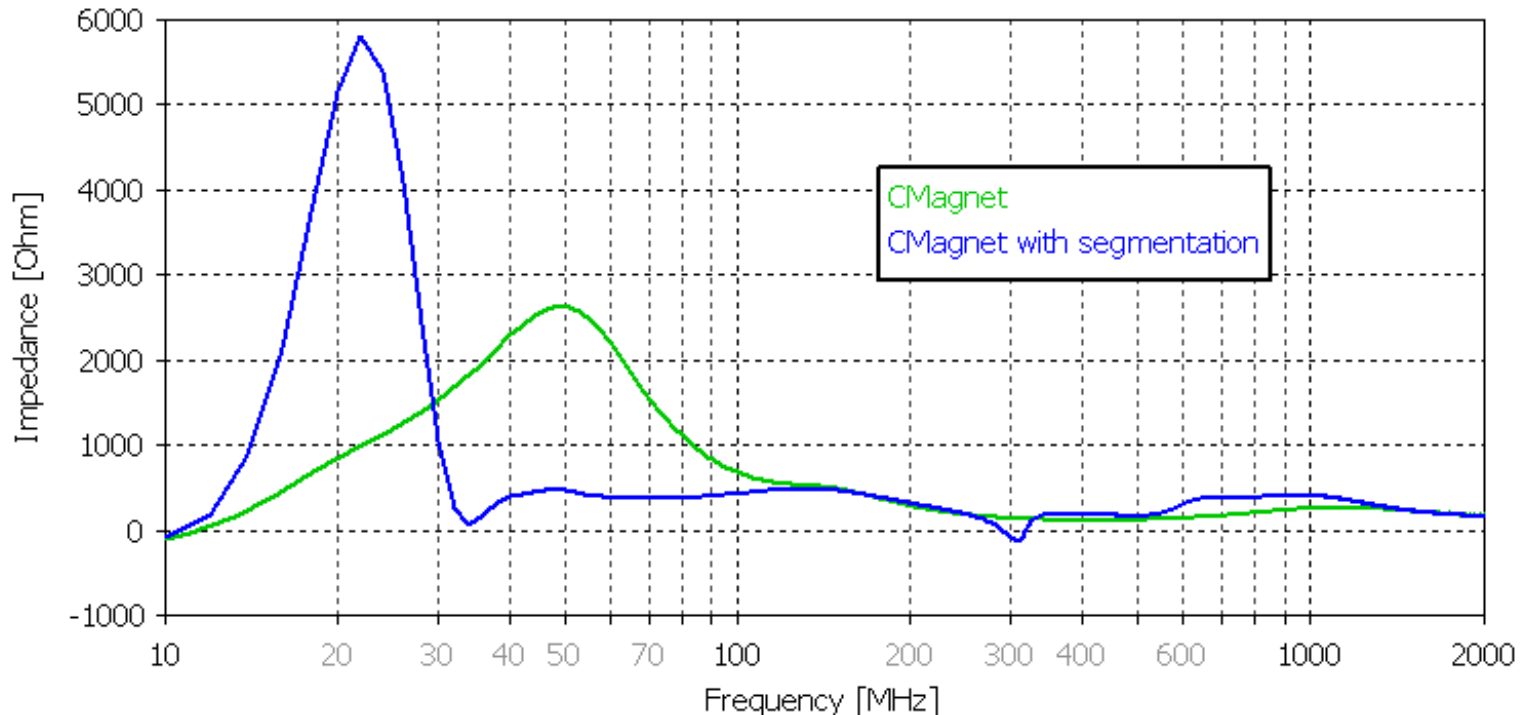
# Overview

- Updated Status of the SPS impedance model
- Improvement of the model
  - Kicker impedance model
    - Status of the SPS kicker impedance model
    - Improvement of the model
      - C-Magnet model
      - Realistic models
      - Comparisons with bench impedance measurements
  - Resistive wall impedance
    - Status of the SPS wall impedance model
    - A more realistic model

# MKP: horizontal transverse impedance

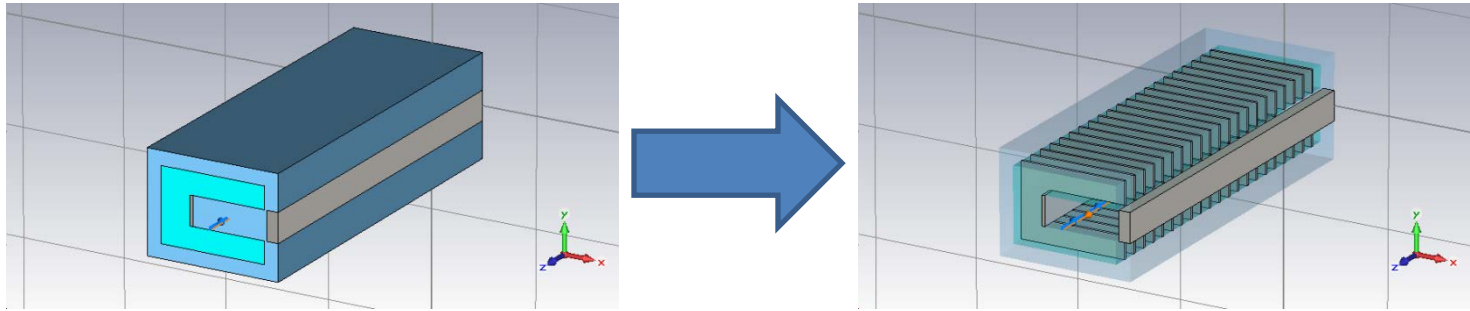


Real horizontal driving impedance calculated at  $x=1\text{cm}$

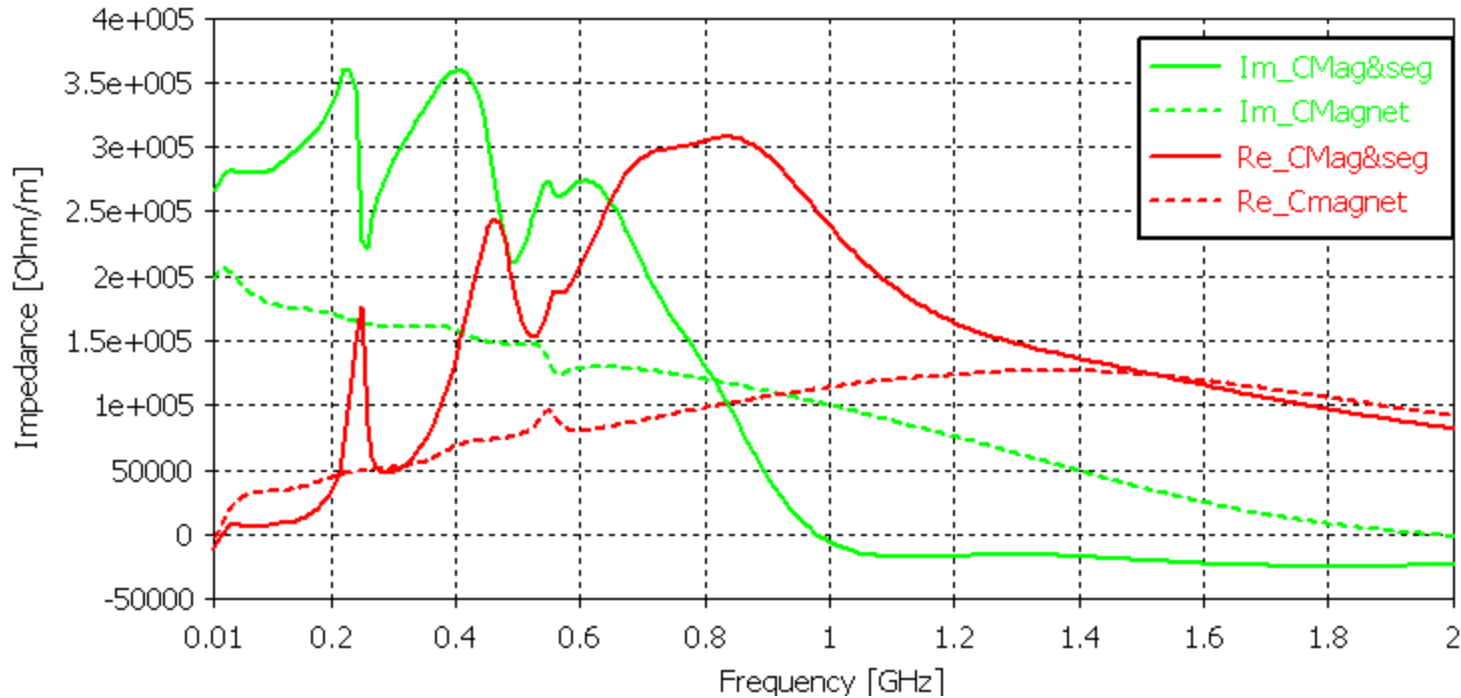


The segmentation seems to affect strongly the TEM peak

# MKP: vertical transverse impedance

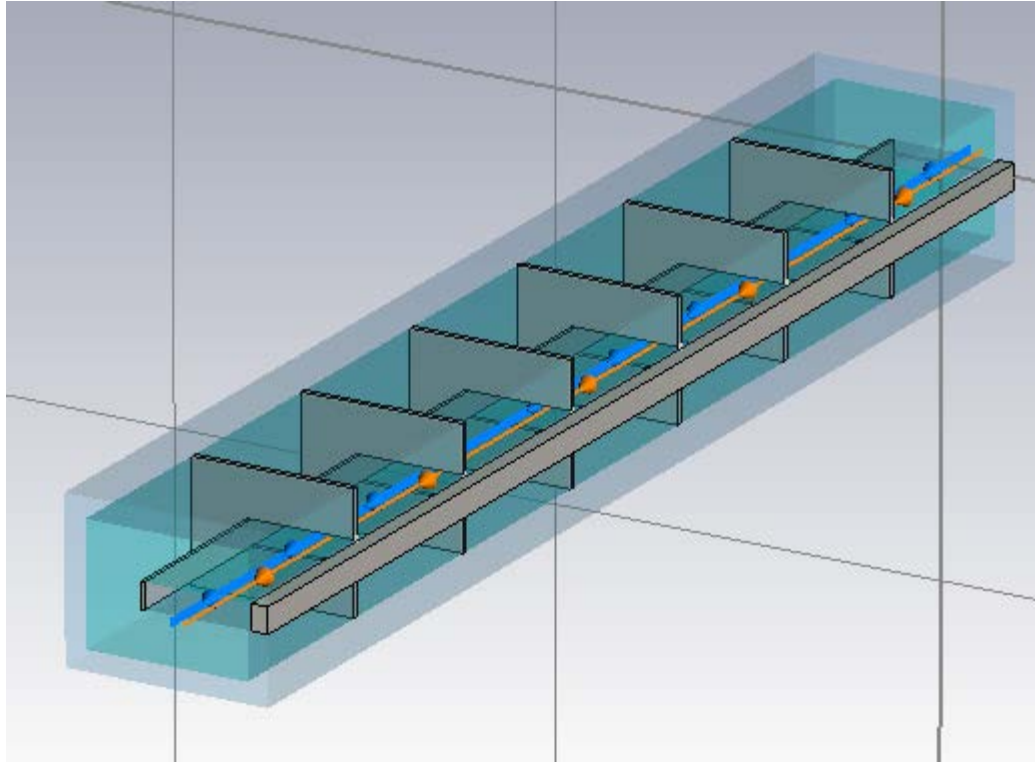


Vertical dipolar impedance



The segmentation has a huge effect on the vertical impedance of the MKP

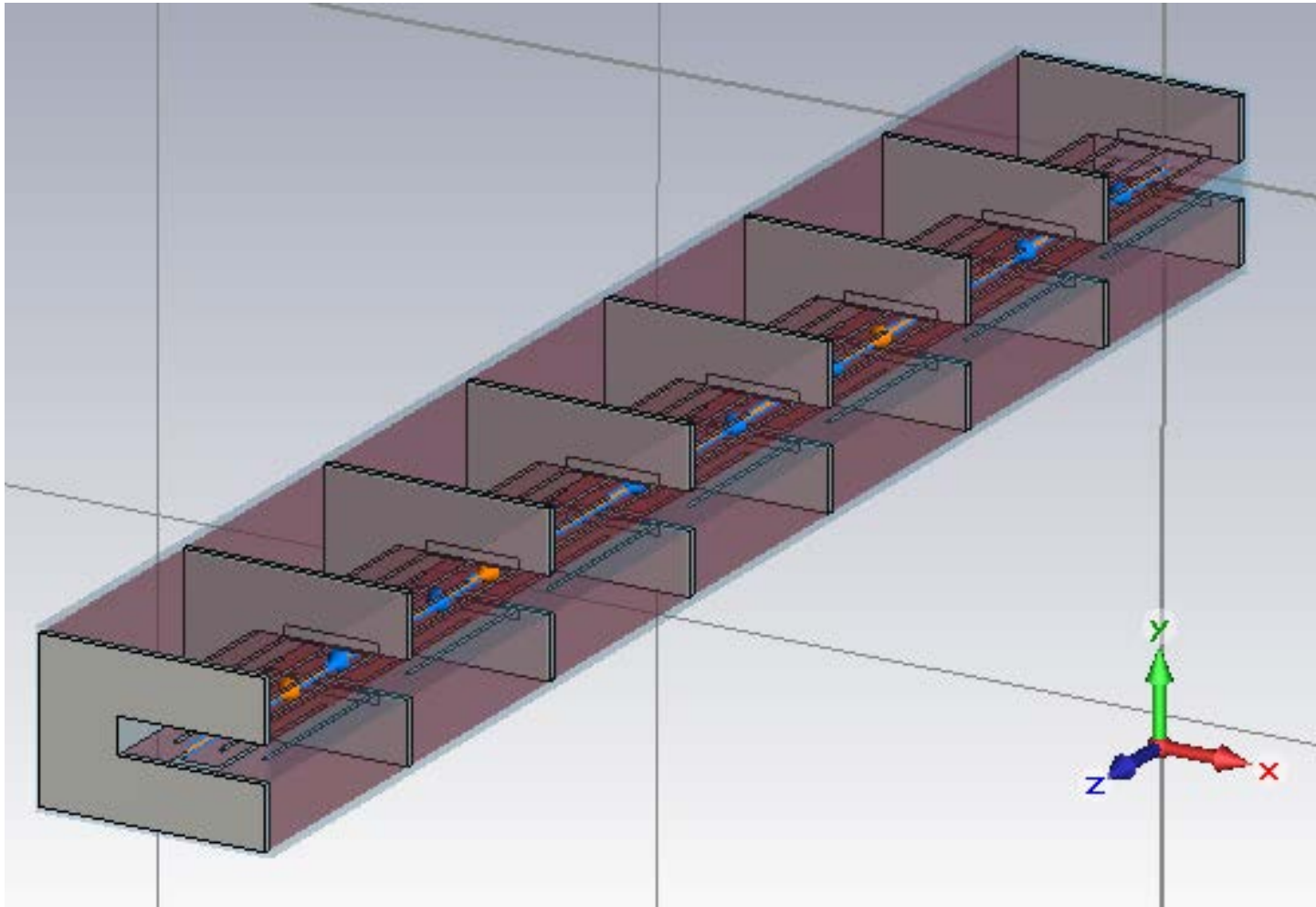
# MKE kickers



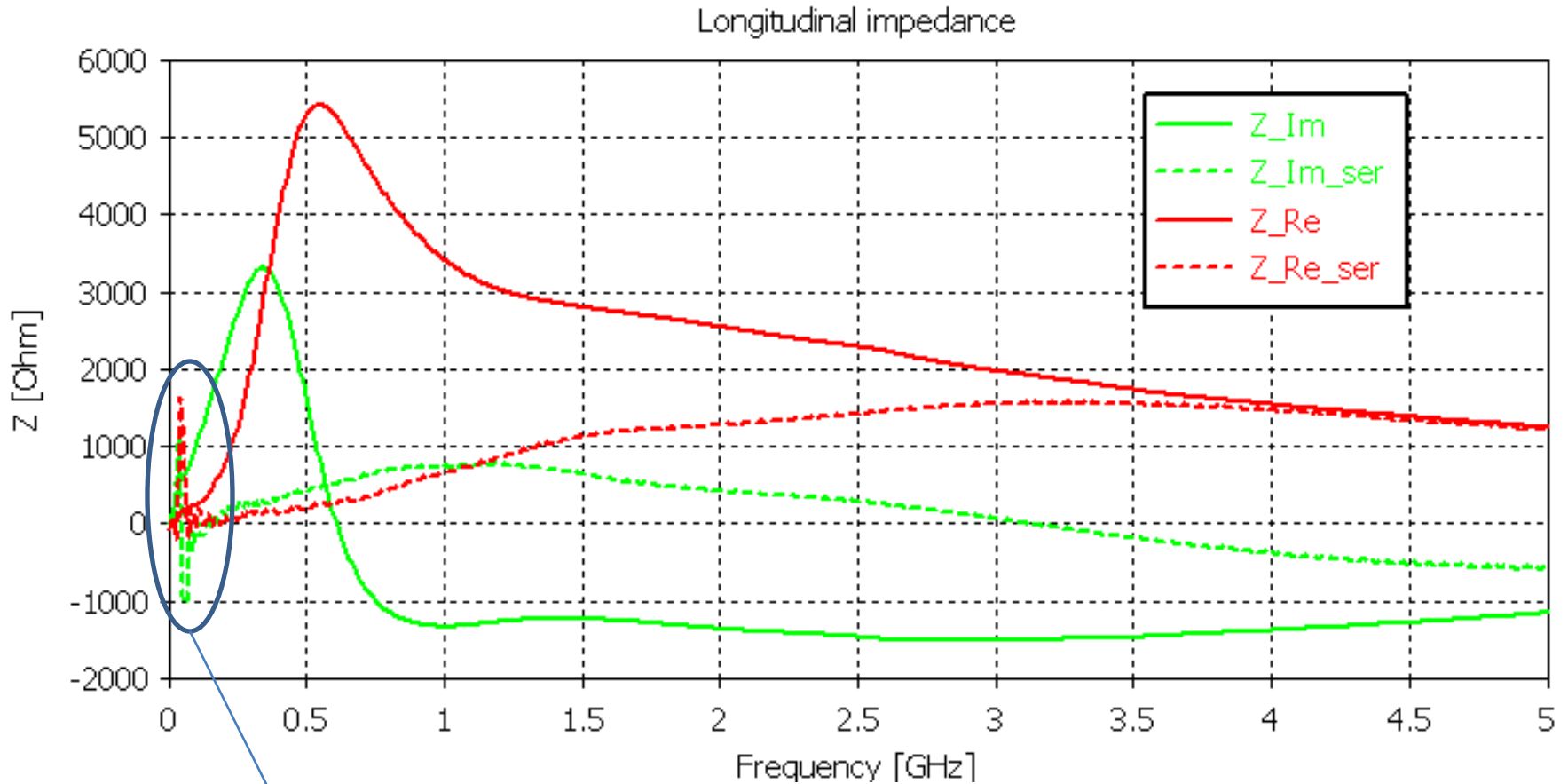
The effect of the segmentation is much less dramatic for the MKE



# MKE kicker with serigraphy



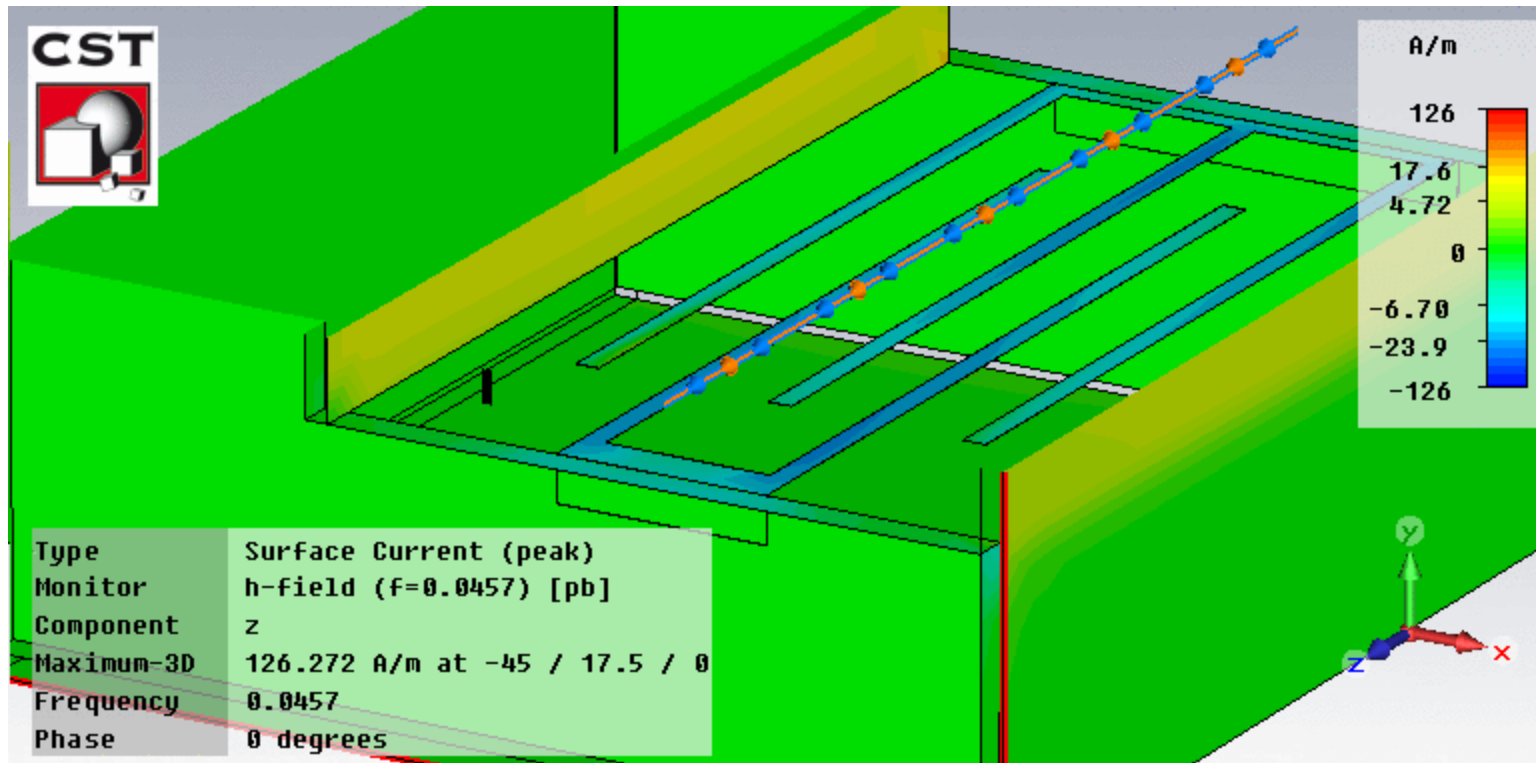
# Comparing MKE with and without serigraphy



$$f=45 \text{ MHz}$$

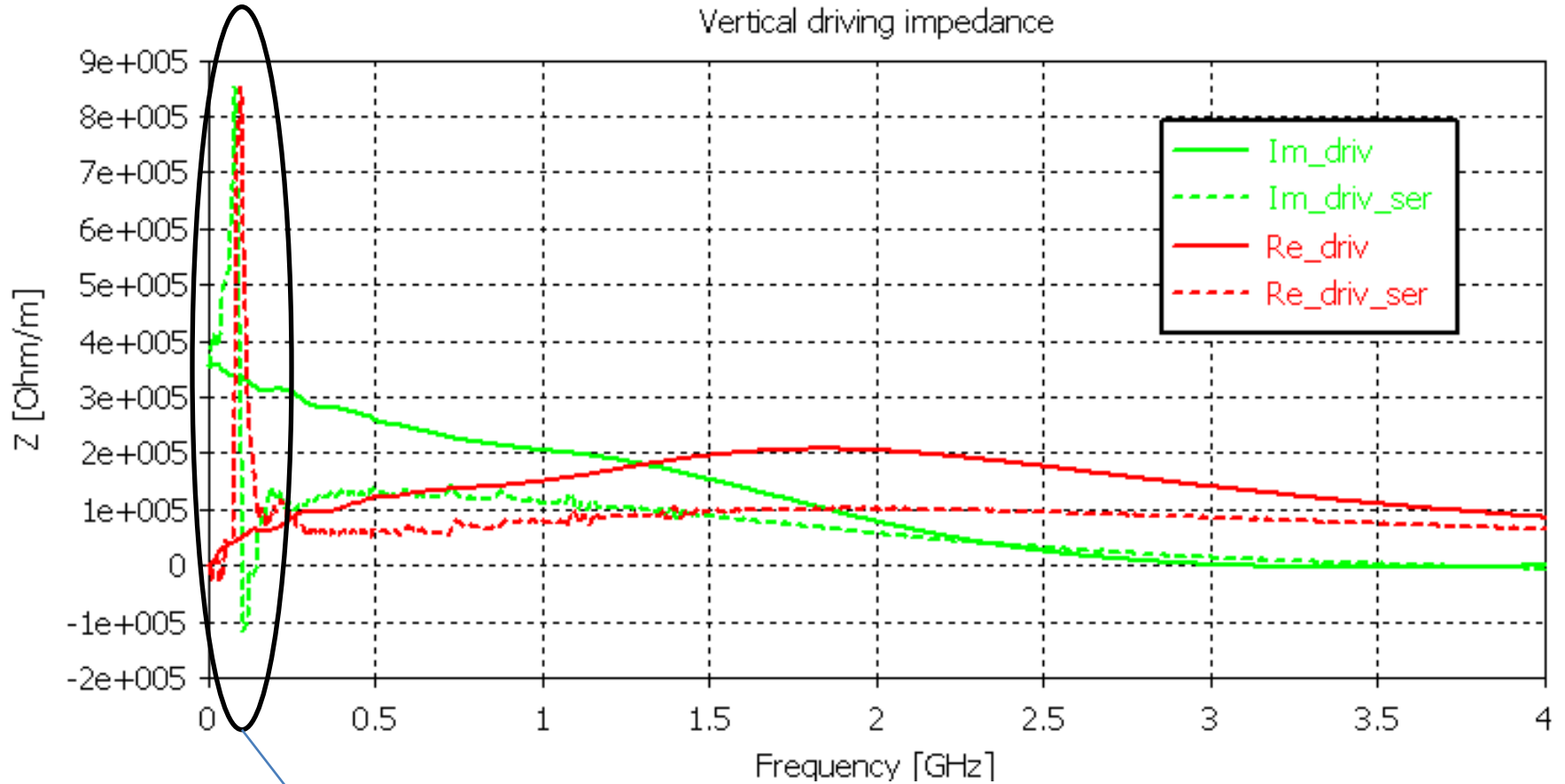
$$\lambda = \frac{c}{f \sqrt{\epsilon_{eff} \mu_{eff}}} \cong 0.78 \text{ m} \cong 4L_{finger}$$

# Comparing MKE with and without serigraphy



The simulation of the EM fields seems to confirm that we have a quarter-wavelength resonance

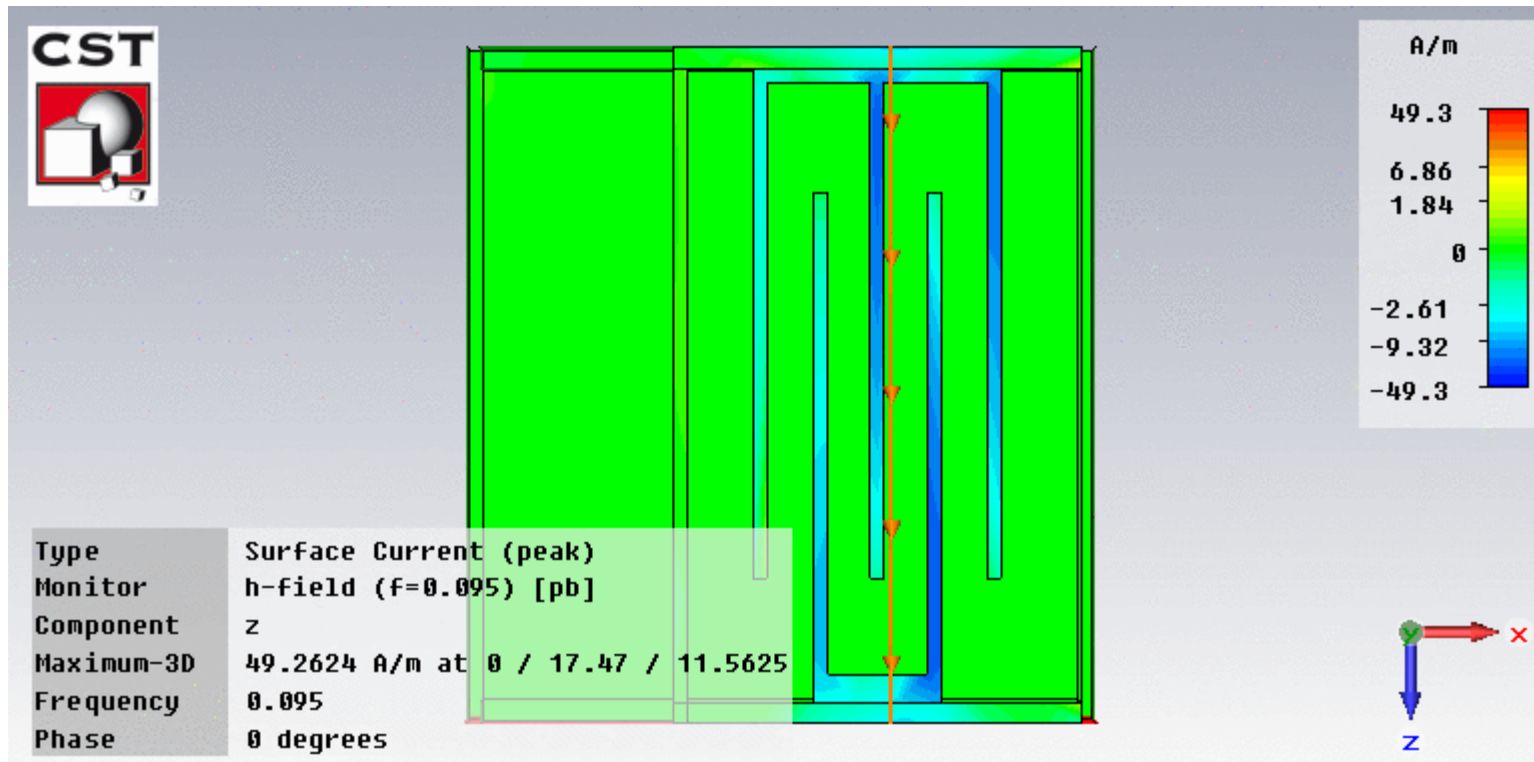
# Comparing MKE with and without serigraphy



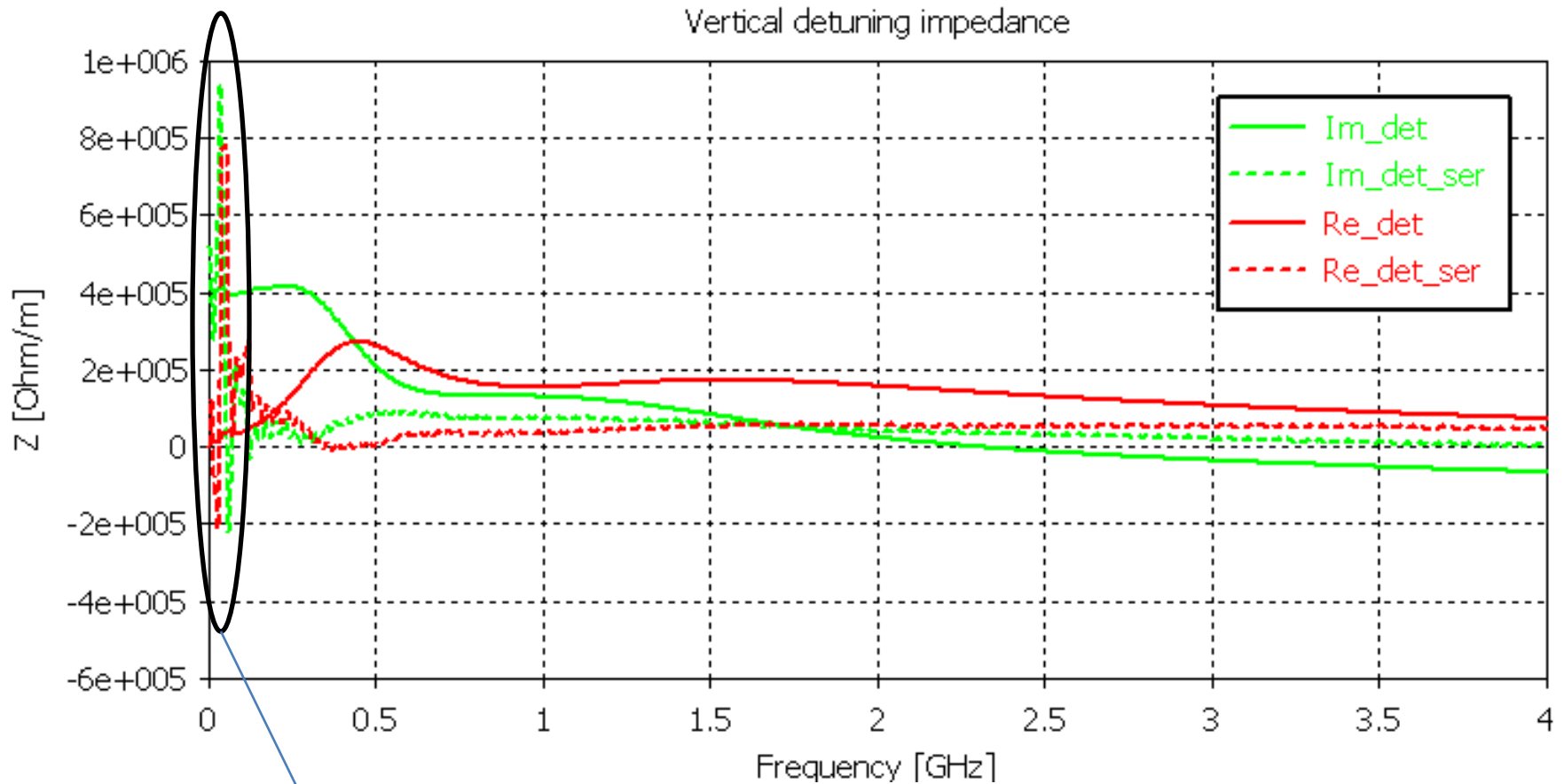
$f=95$  MHz

A resonance of the same nature appears at a frequency double also in the driving transverse impedance

# Comparing MKE with and without serigraphy



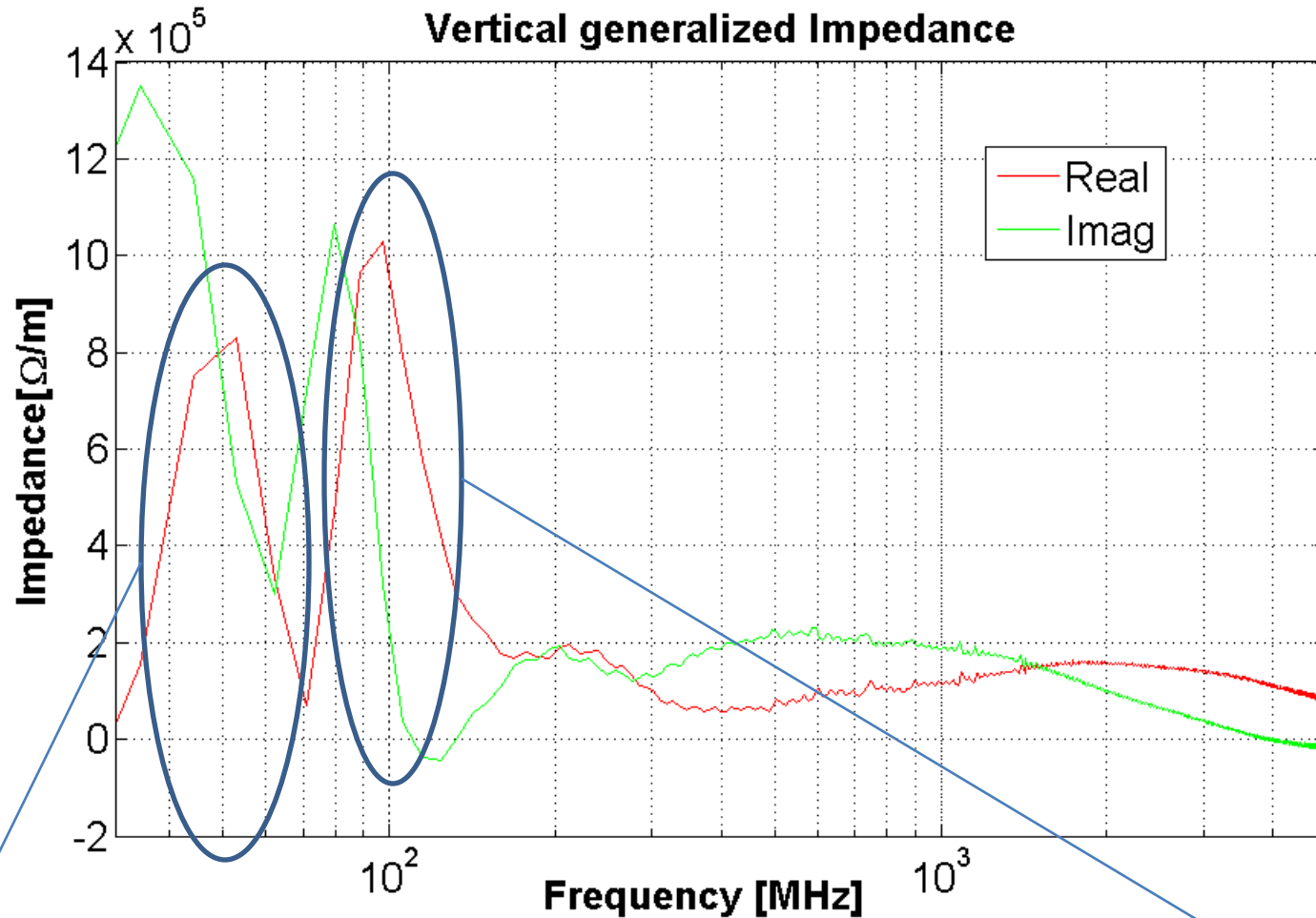
# Comparing MKE with and without serigraphy



$f=45$  MHz

The source is the same as for the longitudinal impedance.

# MKE-L with serigraphy

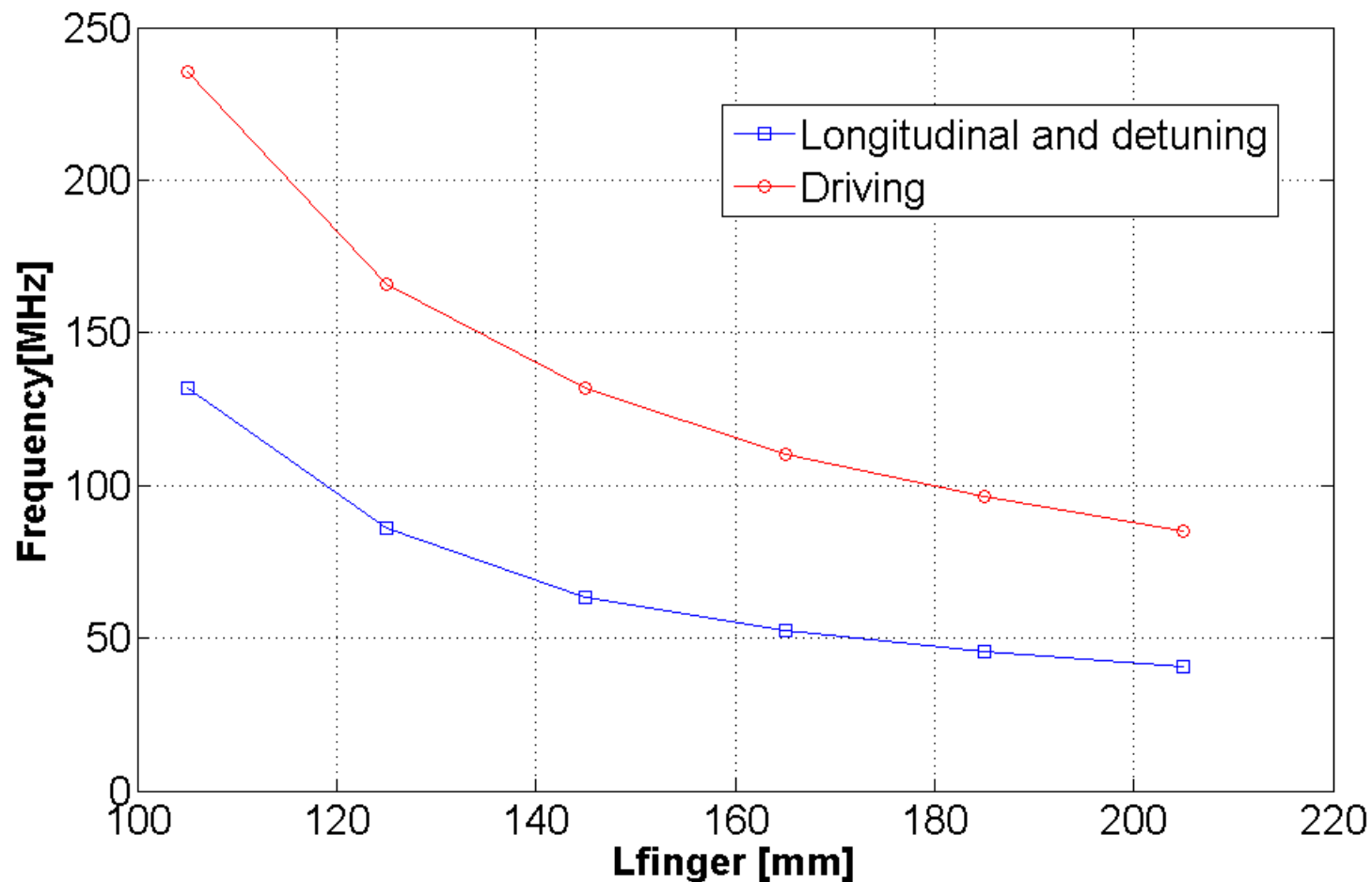


Detuning

Driving

Due to the serigraphy the generalized vertical impedance has two peaks

# Frequency peak versus finger length



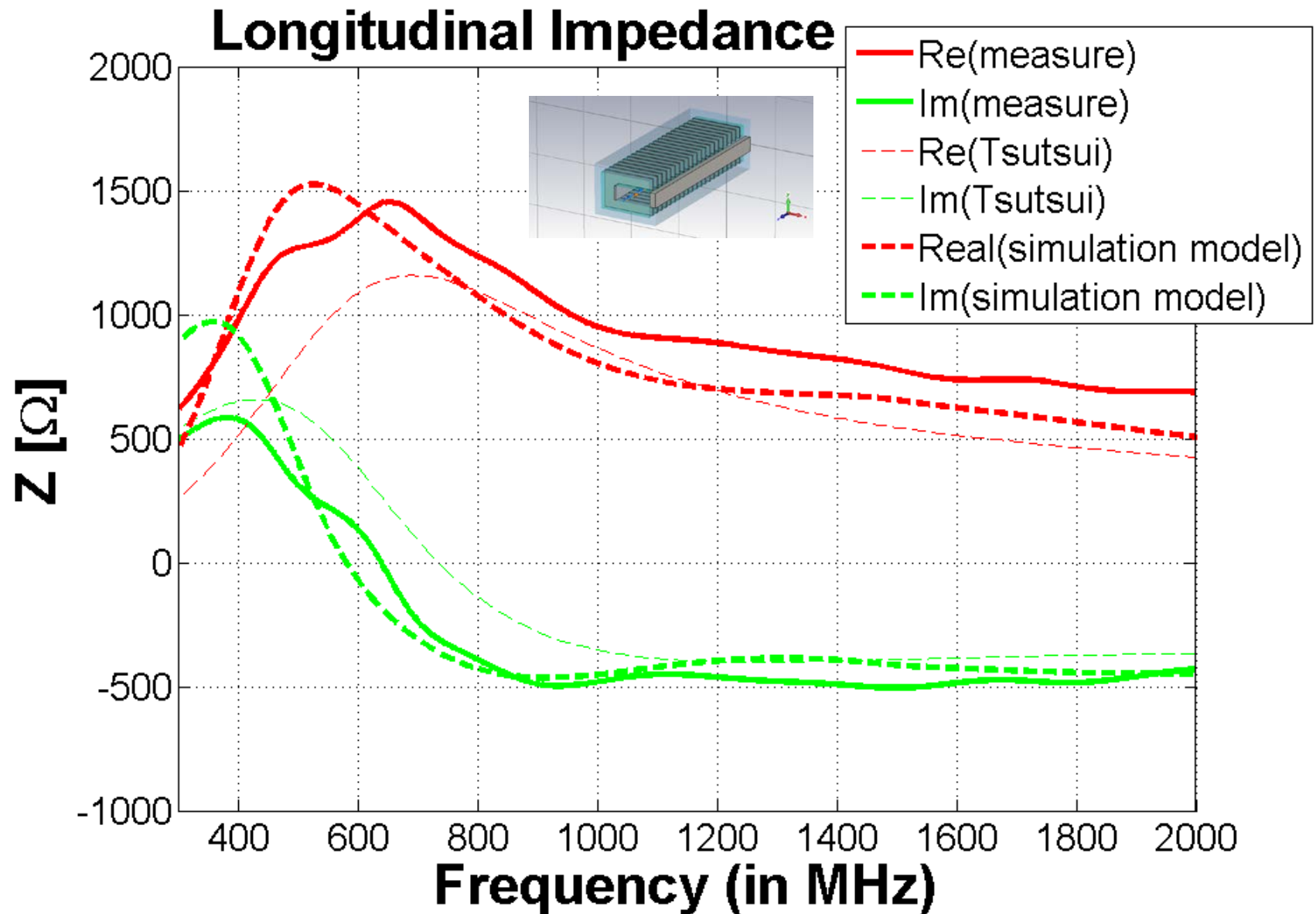
Coherently to what expected the peak strongly depends on the finger length



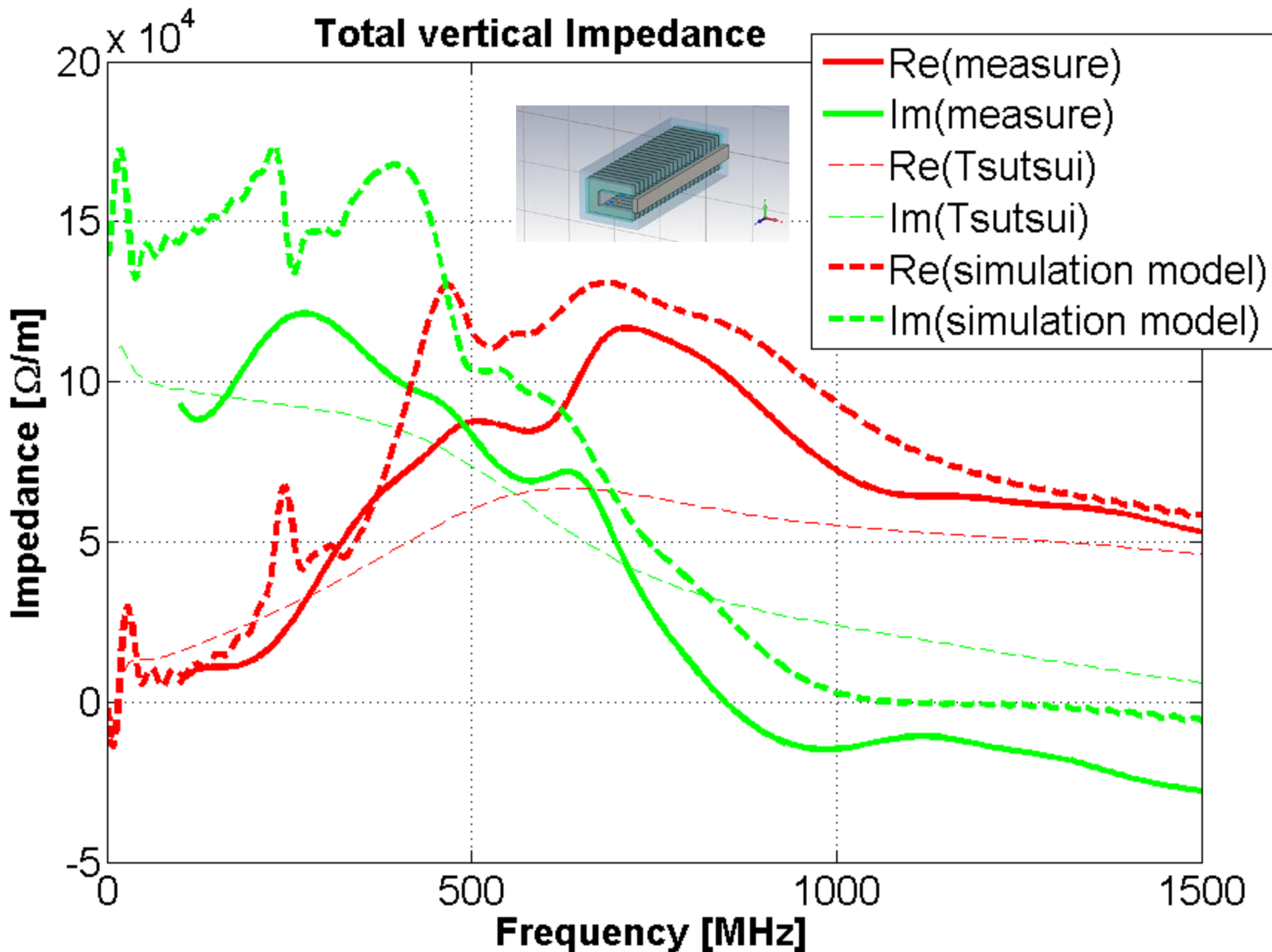
# Overview

- Updated Status of the SPS impedance model
- Improvement of the model
  - Kicker impedance model
    - Status of the SPS kicker impedance model
    - Improvement of the model
      - C-Magnet model
      - Realistic models
      - Comparisons with bench impedance measurements
  - Resistive wall impedance
    - Status of the SPS wall impedance model
    - A more realistic model

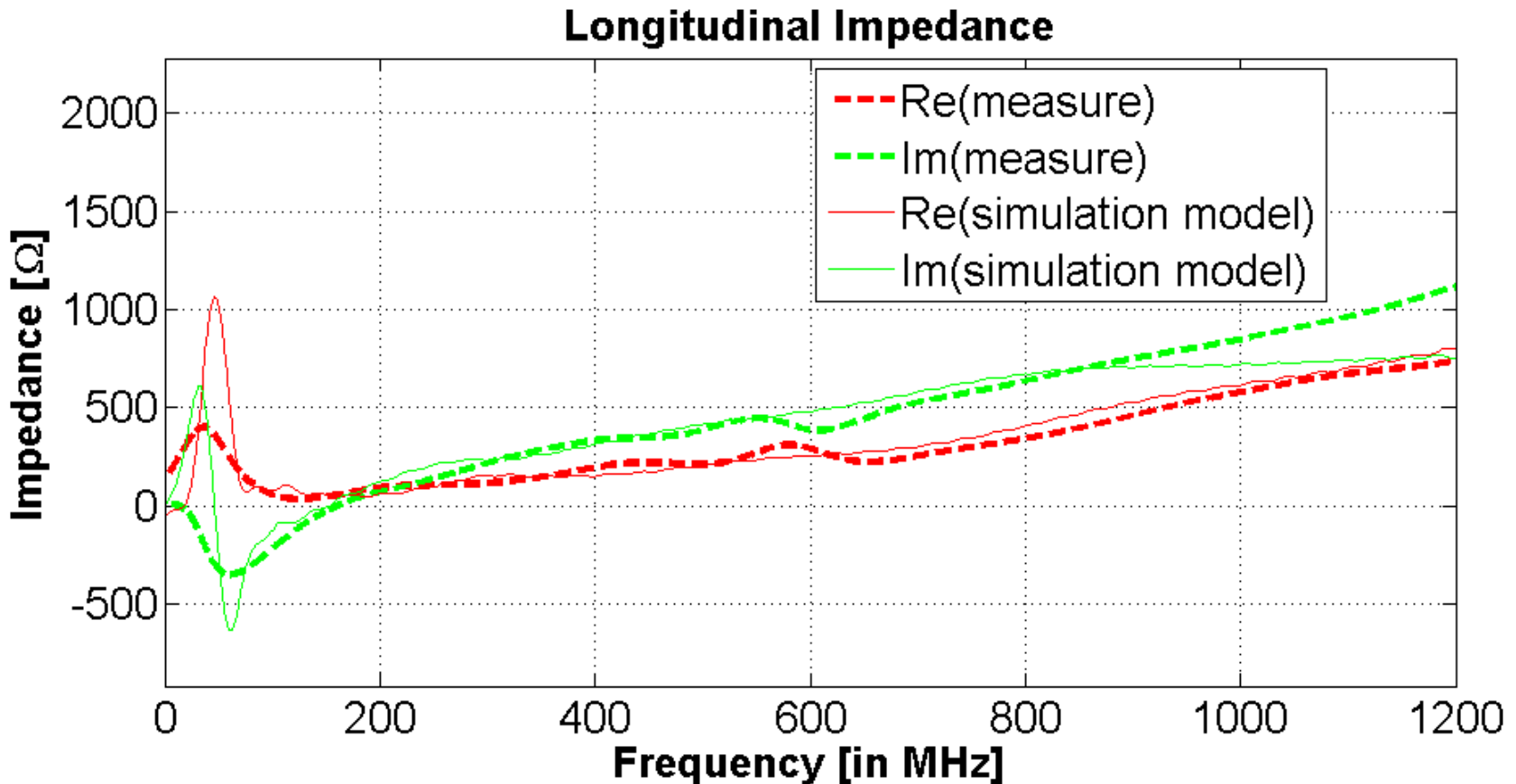
# Comparing longitudinal impedance: MKP-L



# Comparing total transverse impedance: MKP-L

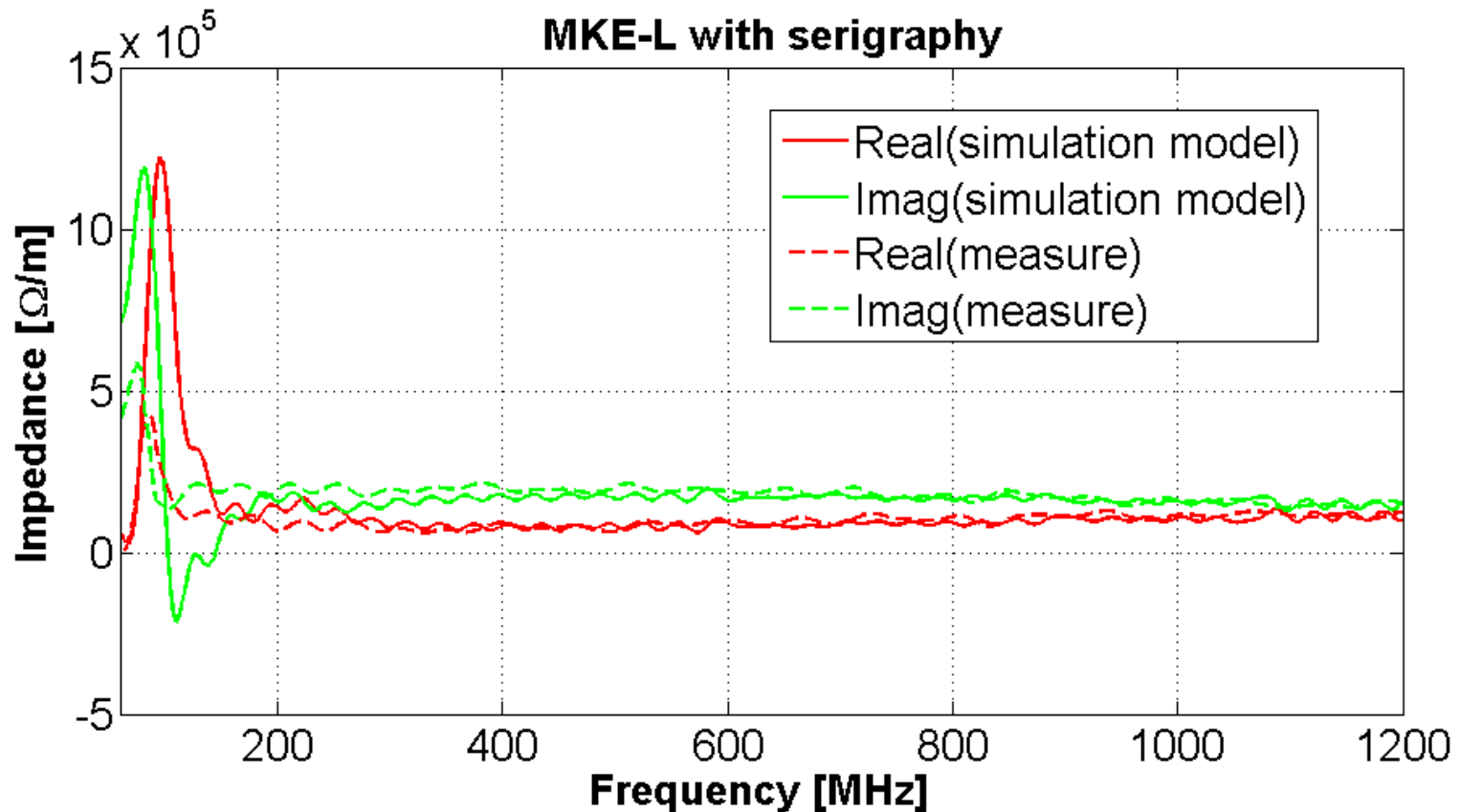


# Comparing longitudinal impedance: MKE-L with serigraphy



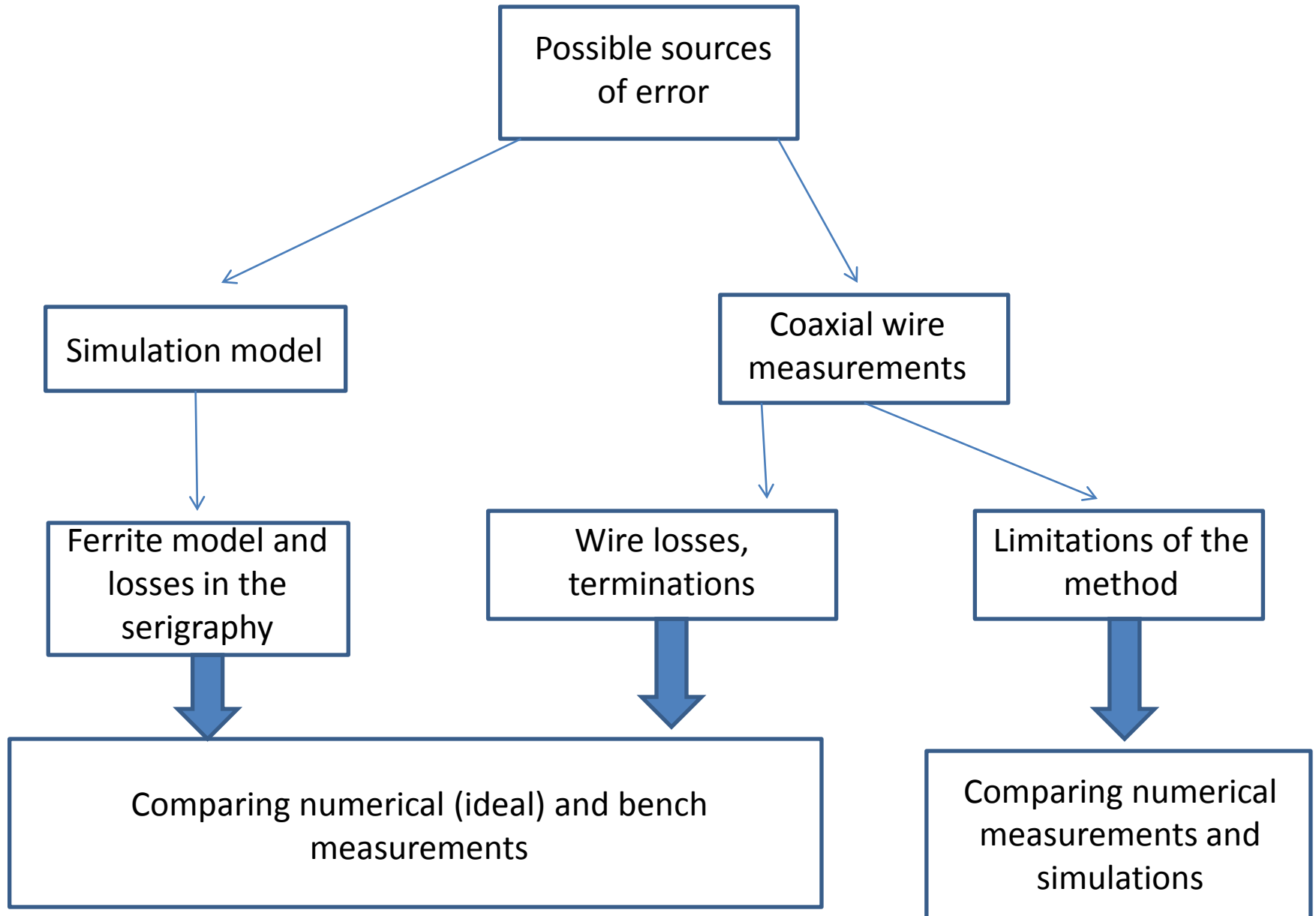
Good agreement except a difference on the low frequency resonance

# Comparing longitudinal impedance: MKE-L with serigraphy

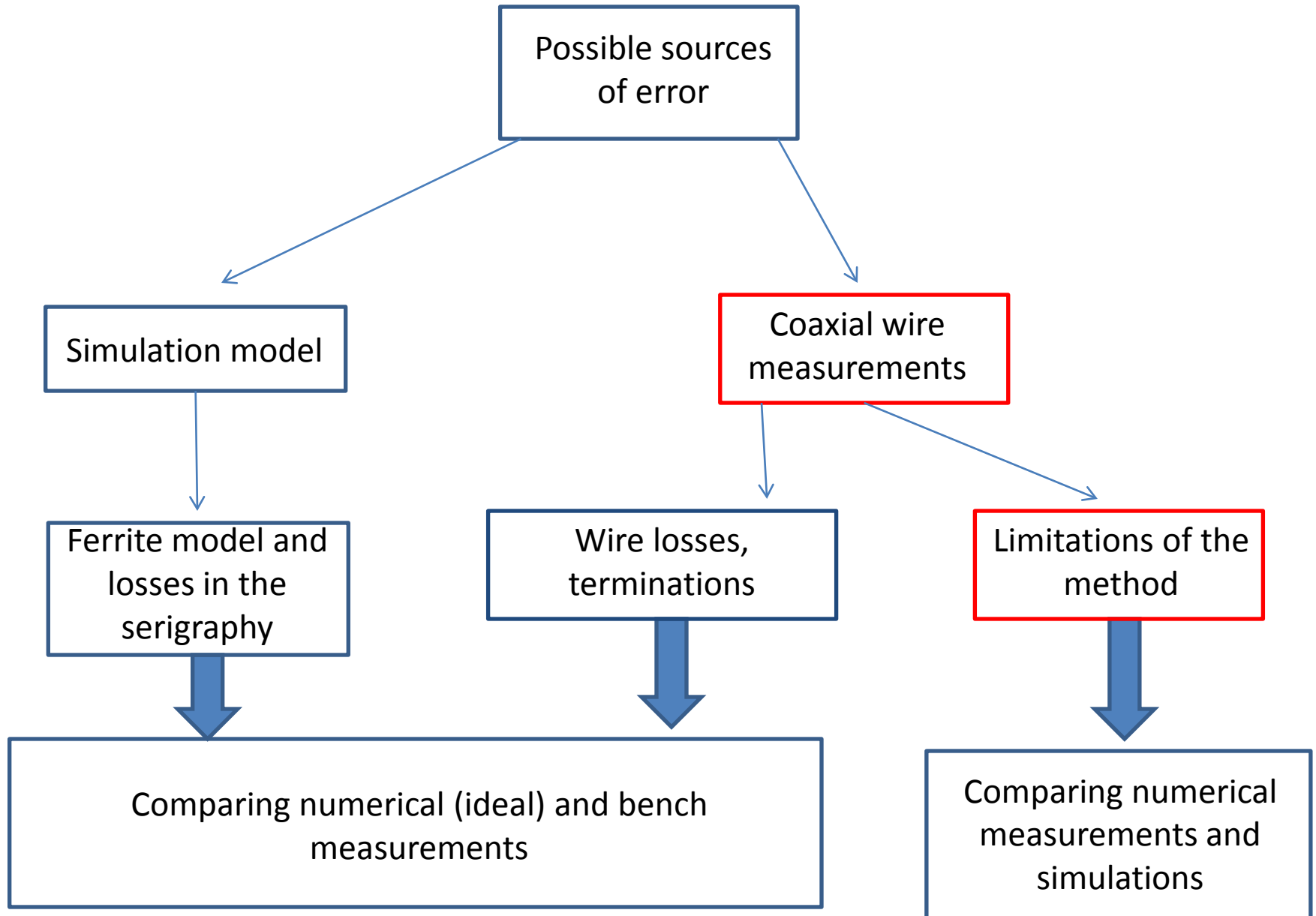


Good agreement except a difference on the low frequency resonance

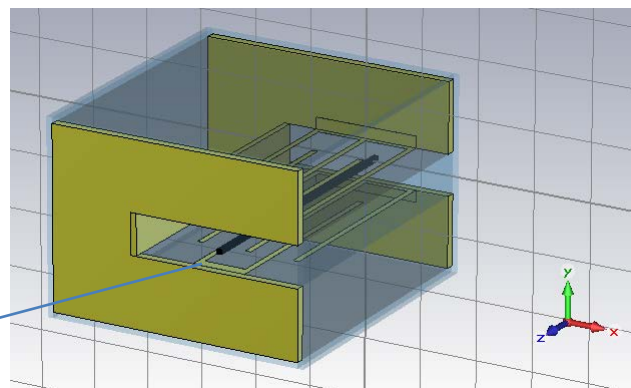
# Investigation of the low frequency discrepancy



# Investigation of the low frequency discrepancy



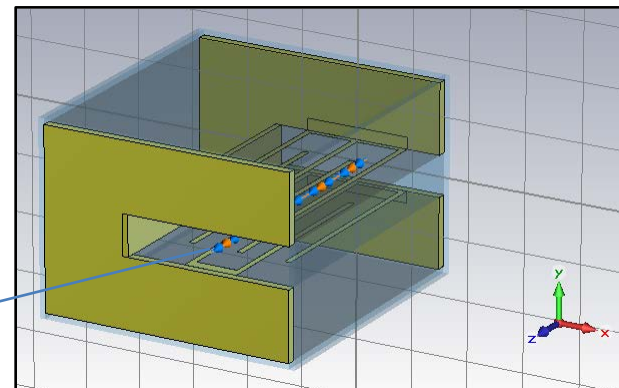
# Comparing numerical measurements and simulations



wire

Simulation output:  $S_{21}$  and  $Z_{ch}$

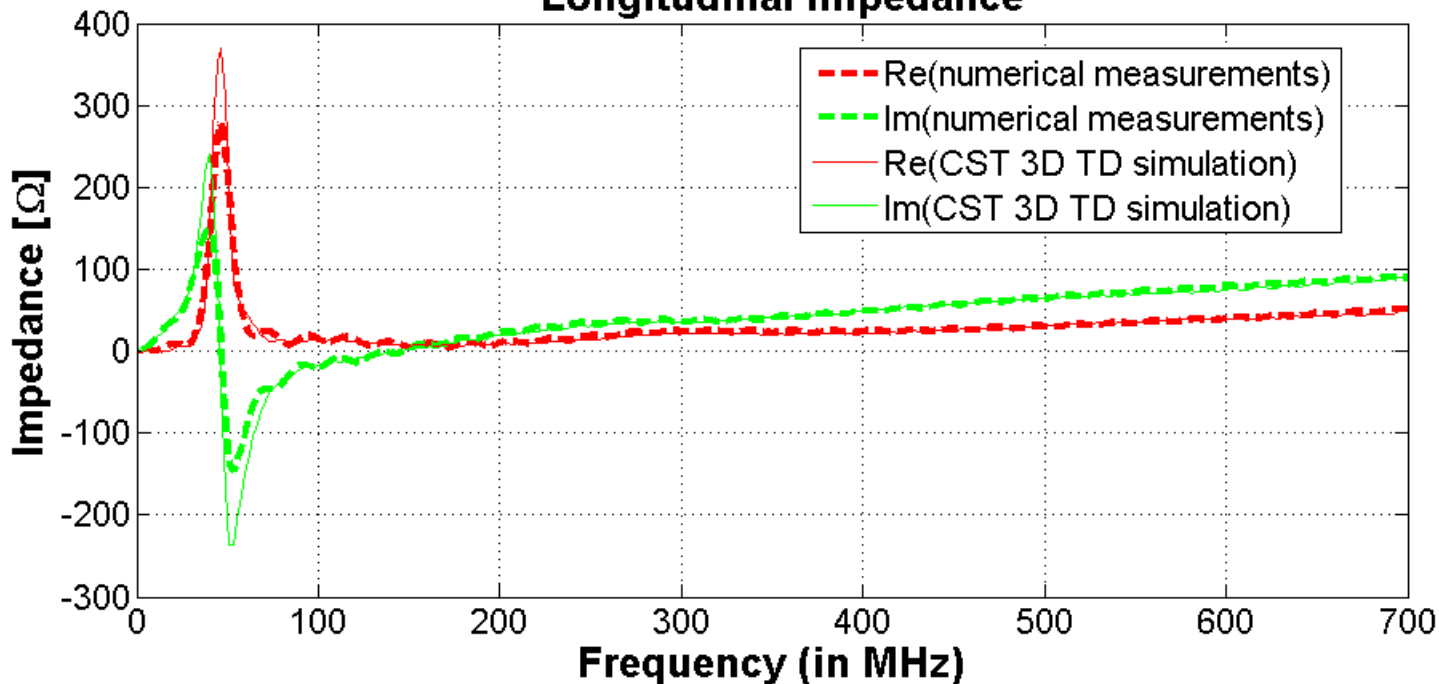
$$Z_{||} = -2Z_{ch} \log\left(\frac{S_{21}}{S_{REF}}\right) \quad S_{REF} = e^{-j\frac{2\pi fL}{c}}$$



beam

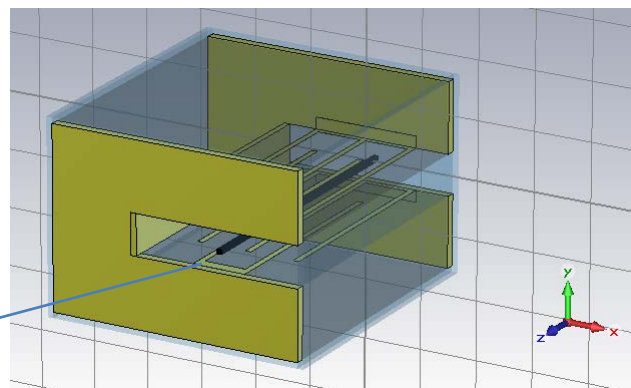
Simulation output: Impedance

## Longitudinal Impedance





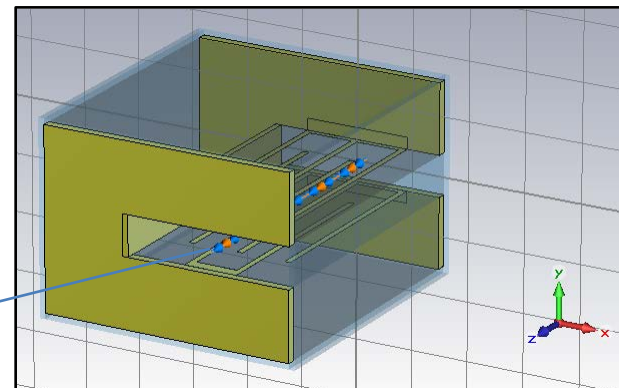
# Comparing numerical measurements and simulations



wire

Simulation output:  $S_{21}$  and  $Z_{ch}$

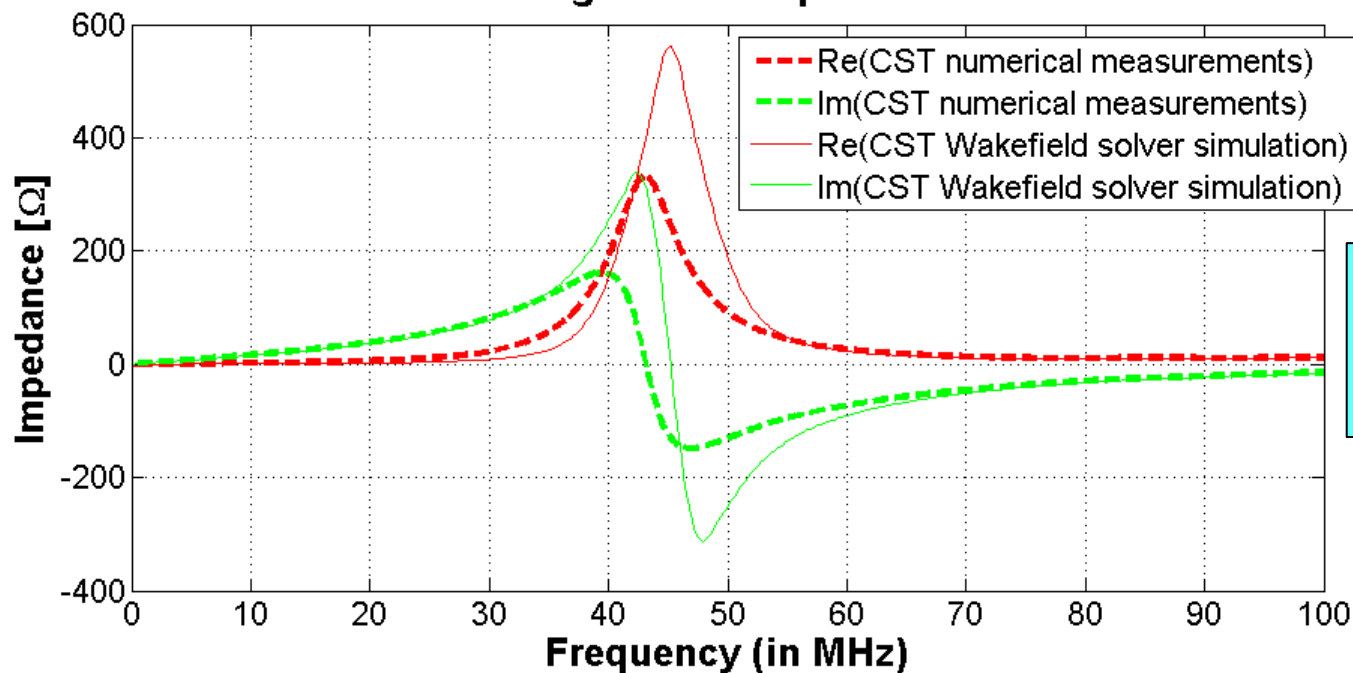
$$Z_{||} = -2Z_{ch} \log\left(\frac{S_{21}}{S_{REF}}\right) \quad S_{REF} = e^{-j\frac{2\pi fL}{c}}$$



beam

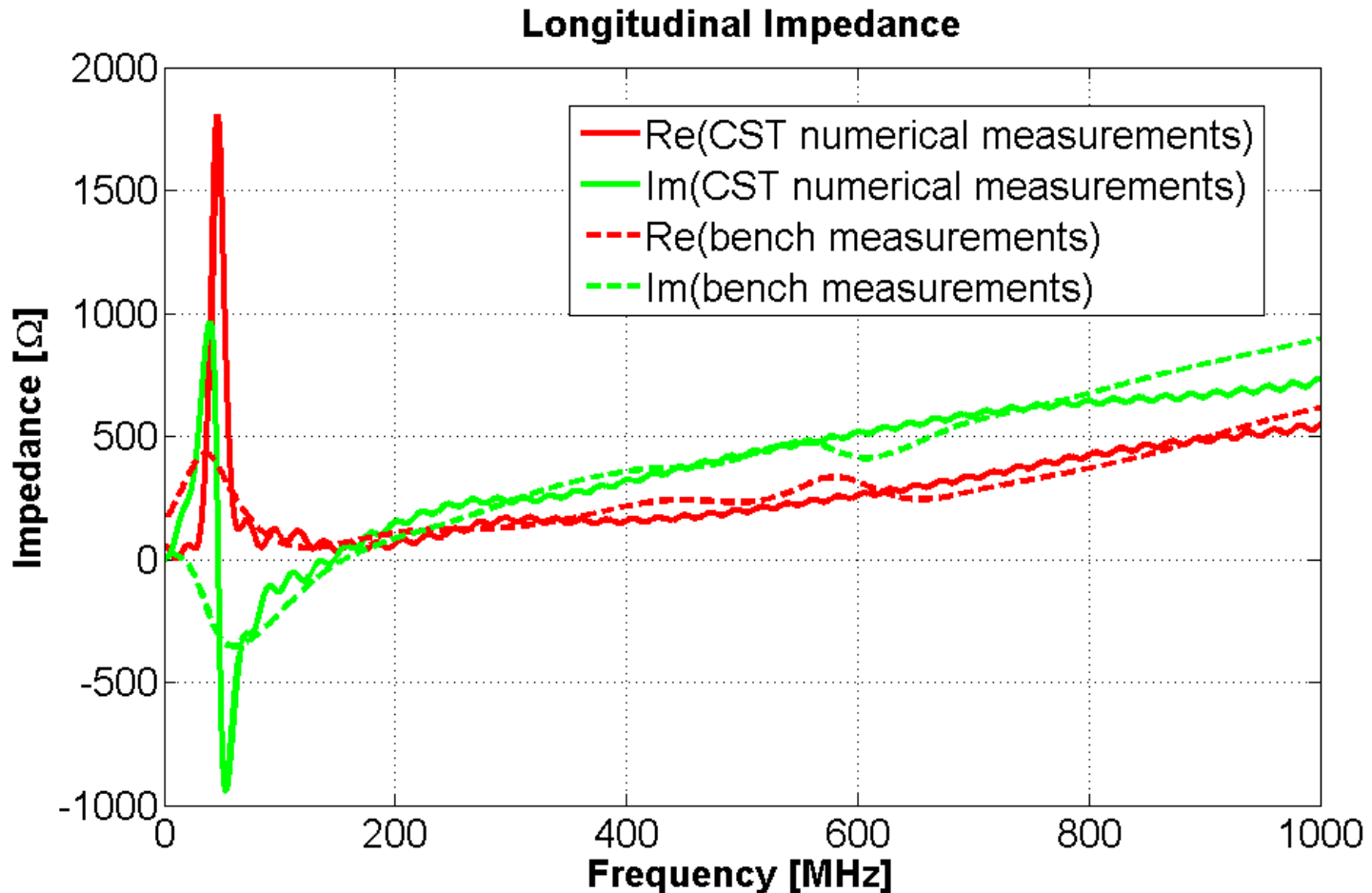
Simulation output: Impedance

## Longitudinal Impedance



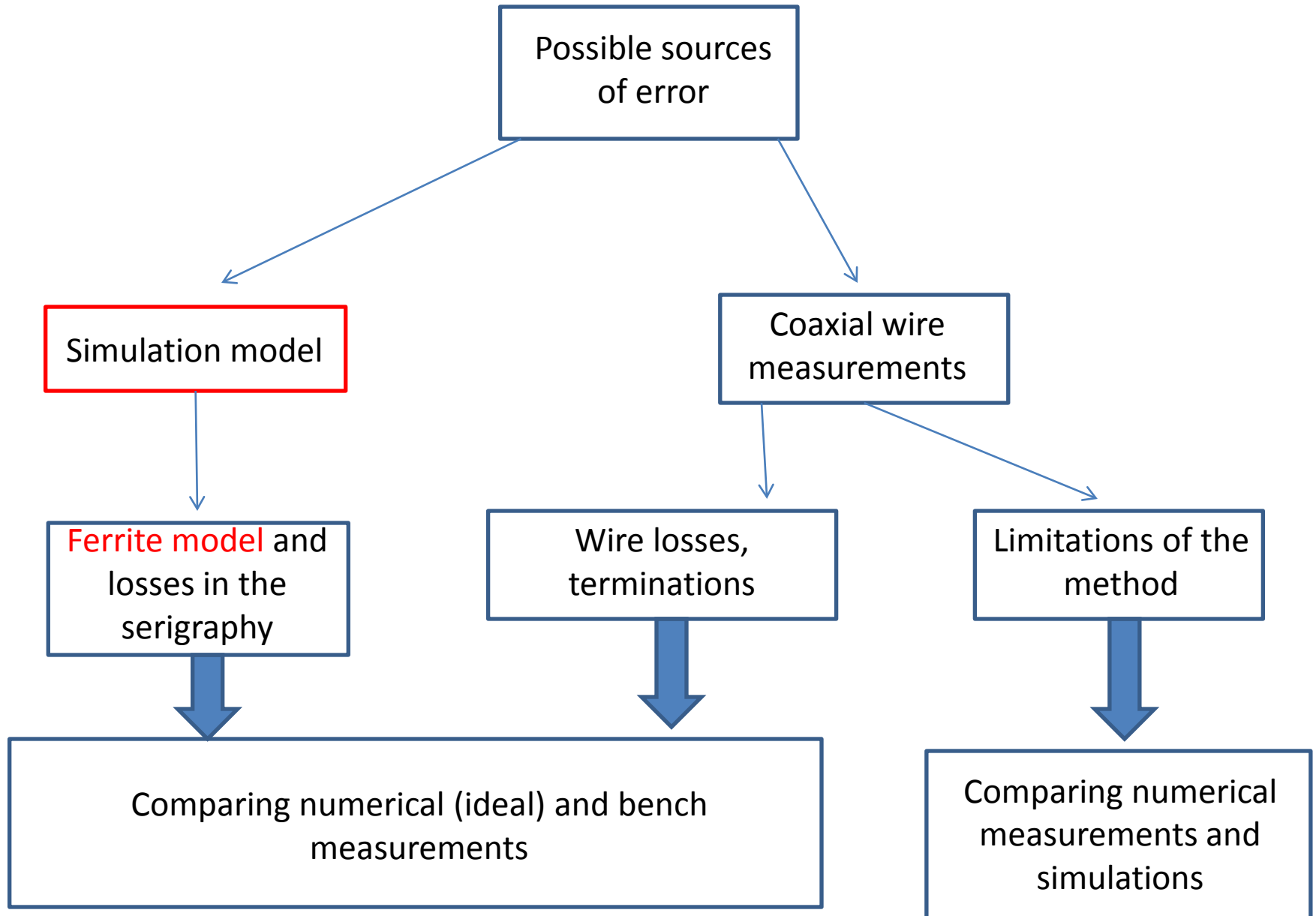
Simulations optimized to investigate the low frequency behaviour

# Comparing numerical and bench measurements



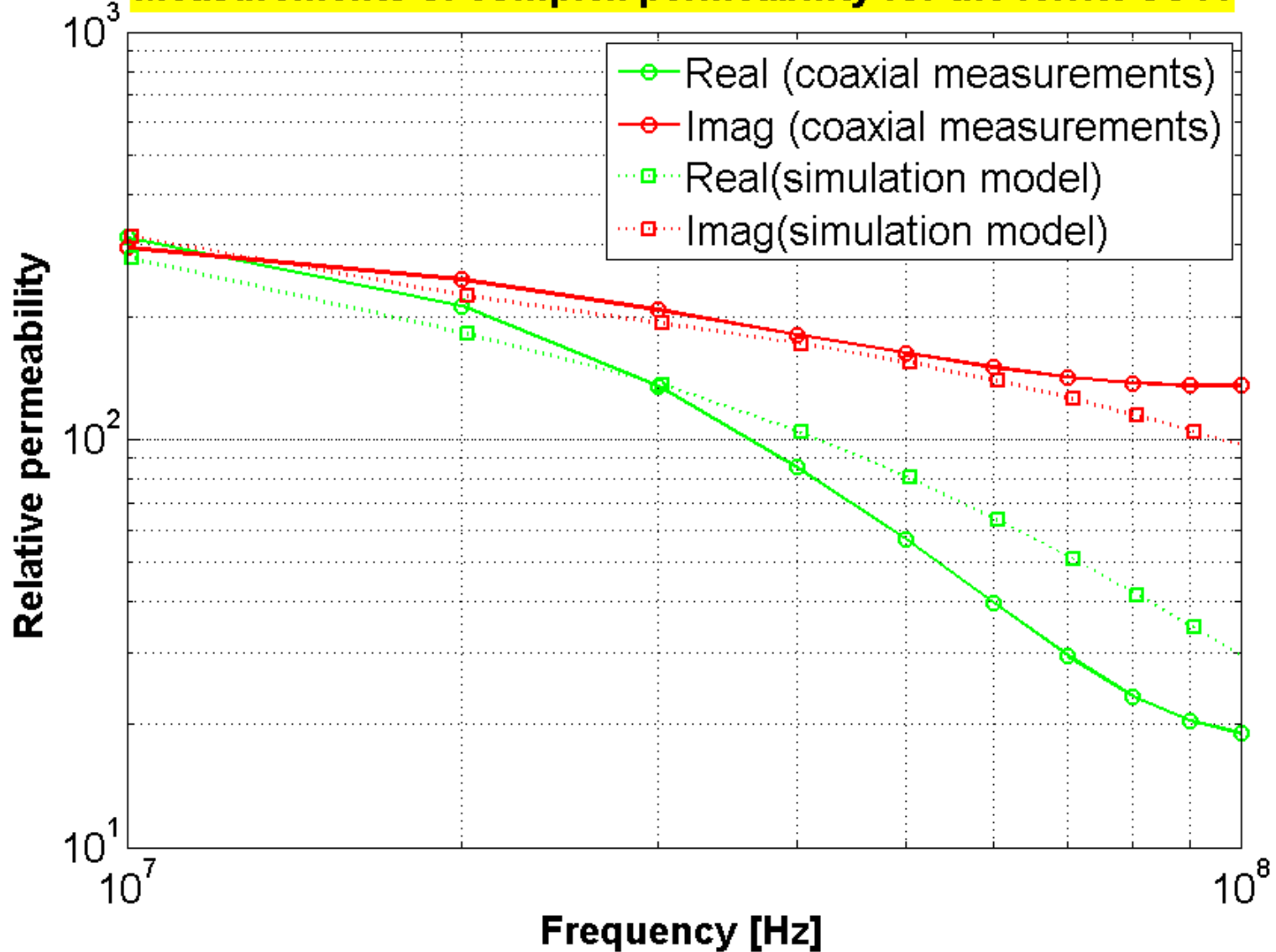
Bench and numerical measurements show a good agreement above a certain frequency but are quite different in the low frequency peak probably due to additional losses in the real setup

# Investigation of the low frequency discrepancy



# Ferrite permeability model

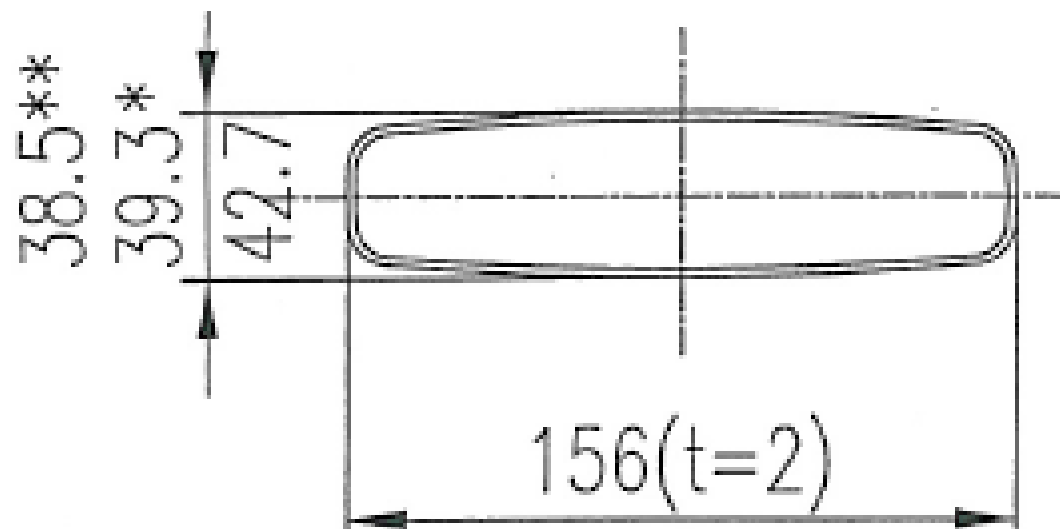
Measurements of complex permeability for the ferrite 8C11



# Overview

- Status of the SPS impedance model
- Improvement of the model
  - Kicker impedance model
    - Status of the SPS kicker impedance model
    - Improvement of the model
      - C-Magnet model
      - Realistic models
      - Comparisons with bench impedance measurements
  - Resistive wall impedance
    - Status of the SPS wall impedance model
    - A more realistic model

# Status of the SPS wall Impedance



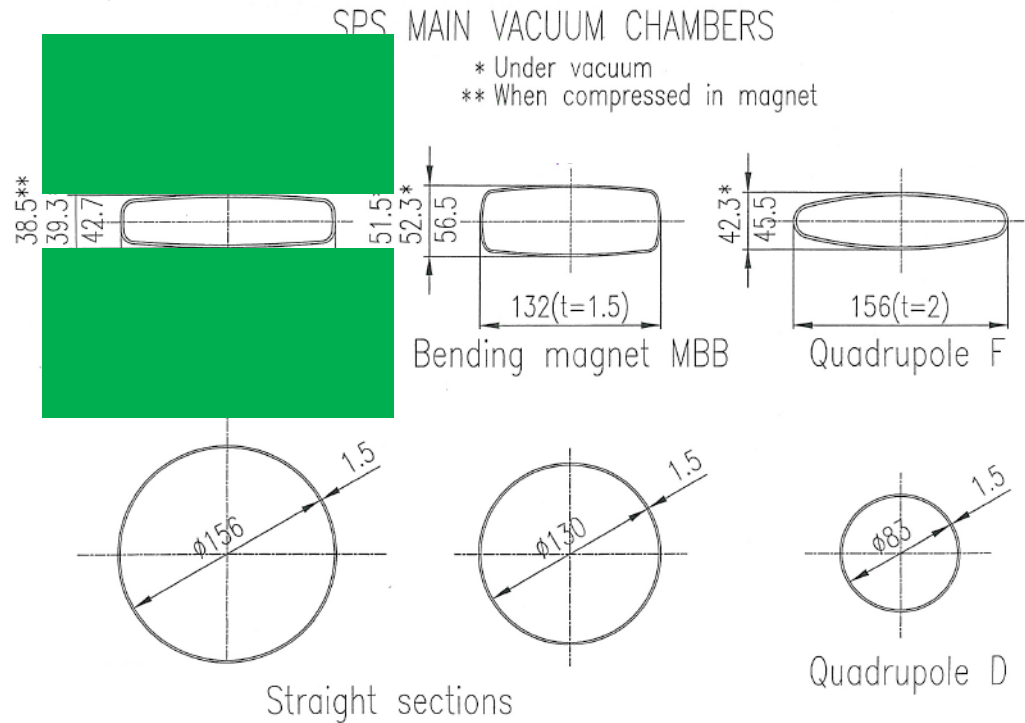
Bending magnet MBA

6.911 km beam pipe (Zotter/Metral analytical calculations for a round pipe of 20mm radius including indirect space charge, transformed with Yokoya factor)

# Overview

- Status of the SPS impedance model
- Improvement of the model
  - Kicker impedance model
    - Status of the SPS kicker impedance model
    - Improvement of the model
      - C-Magnet model
      - Realistic models
      - Comparisons with bench impedance measurements
  - Resistive wall impedance
    - Status of the SPS wall impedance model
    - A more realistic model

# Improvement of the model



$$Z_x = \frac{1}{\langle \beta_x \rangle} \sum_{i=1}^6 Z_{xi} L_i \langle \beta_{xi} \rangle$$

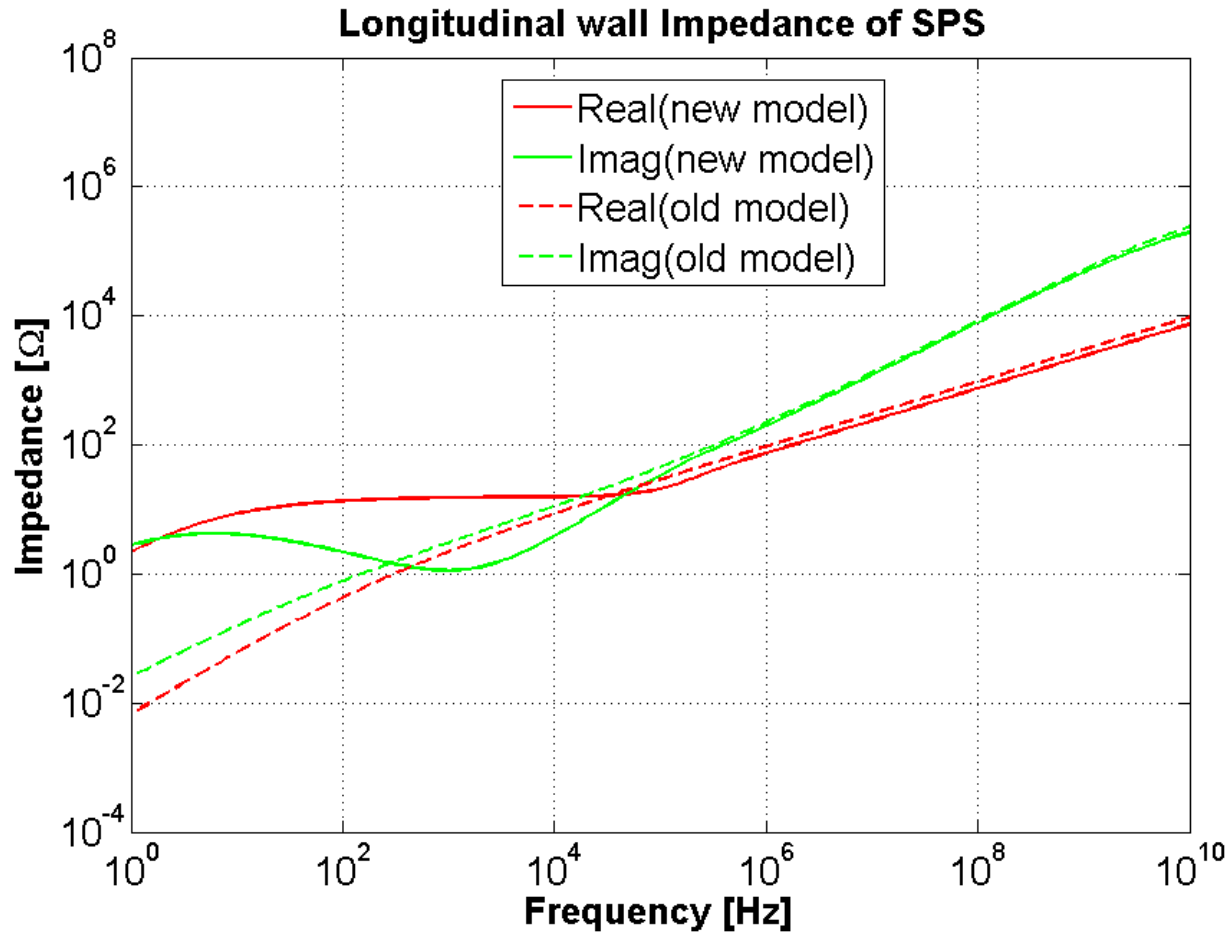
$$Z_y = \frac{1}{\langle \beta_y \rangle} \sum_{i=1}^6 Z_{yi} L_i \langle \beta_{yi} \rangle$$

$$Z_l = \sum_{i=1}^6 Z_{li} L_i$$

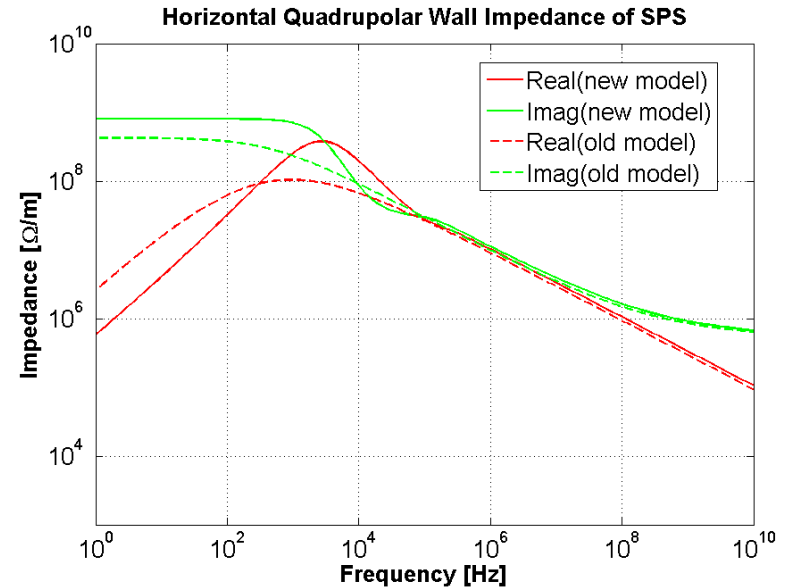
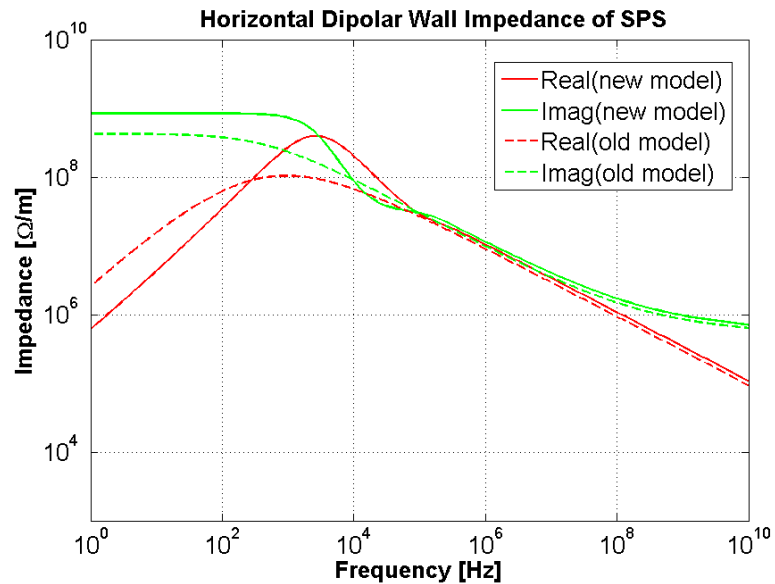
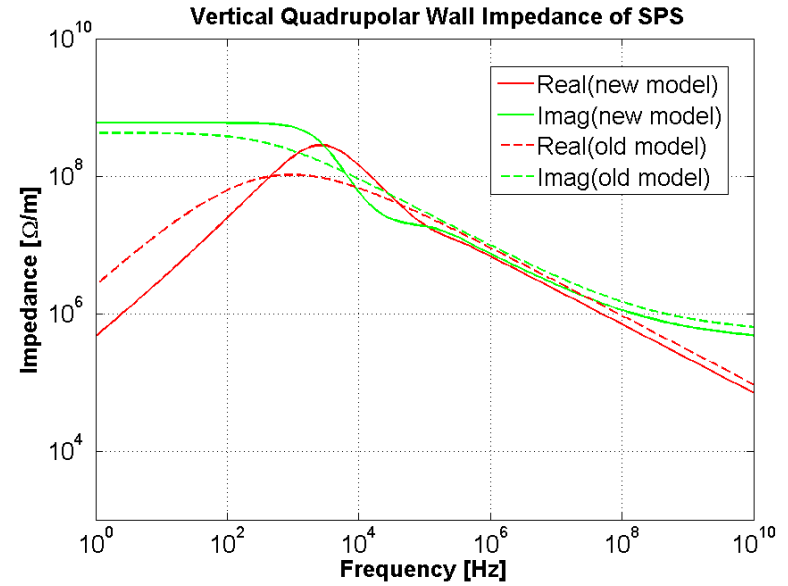
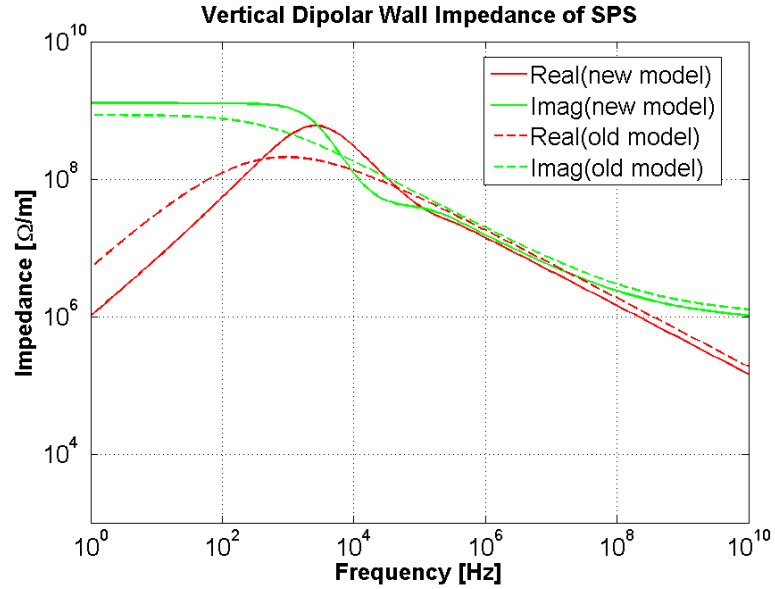
1. Different vacuum chambers weighted by the respective length and beta function
2. The iron in the magnets is also taken into account



# Longitudinal Impedance



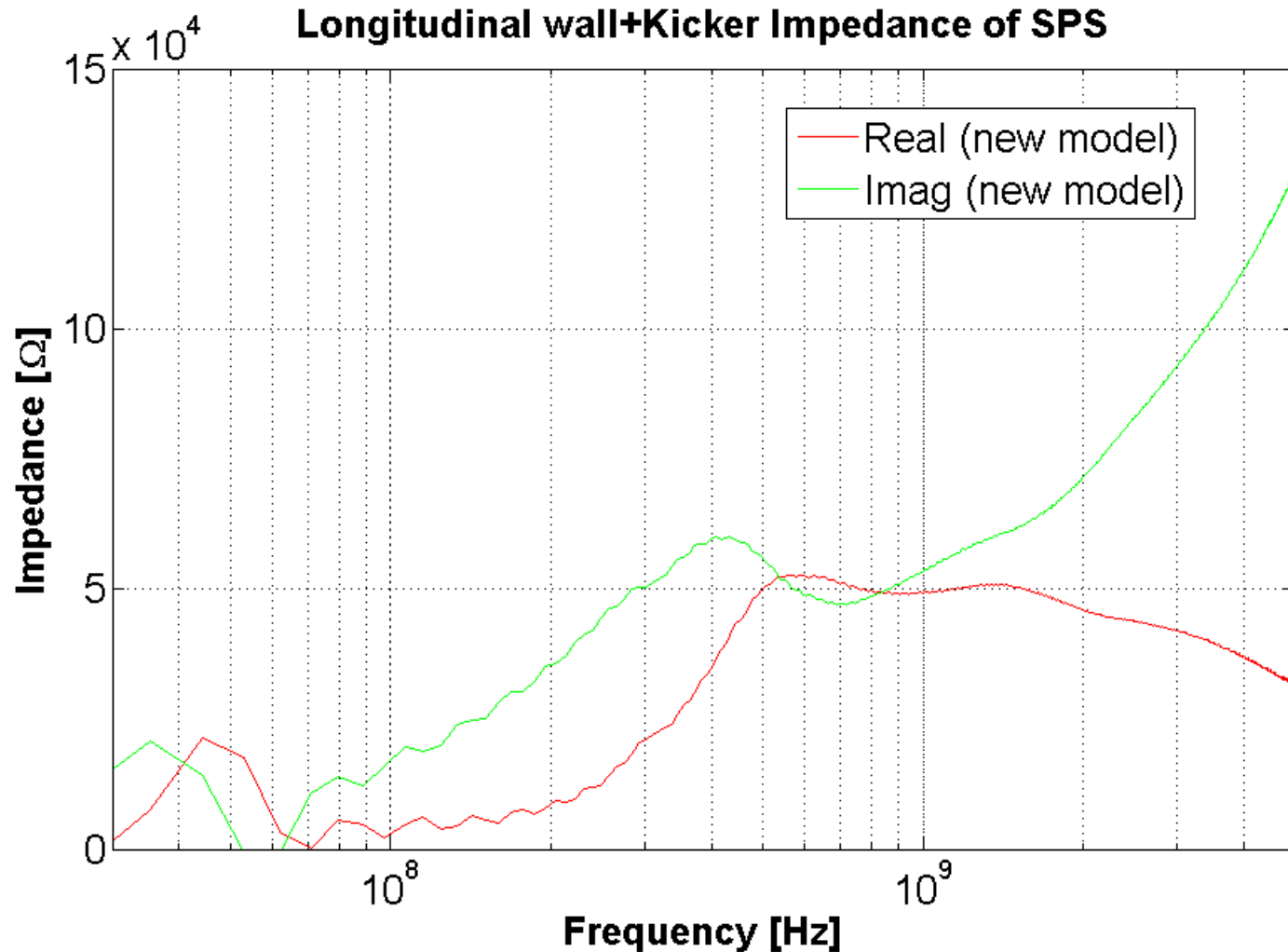
# Transverse Impedance: Q26 Optics



# Conclusions

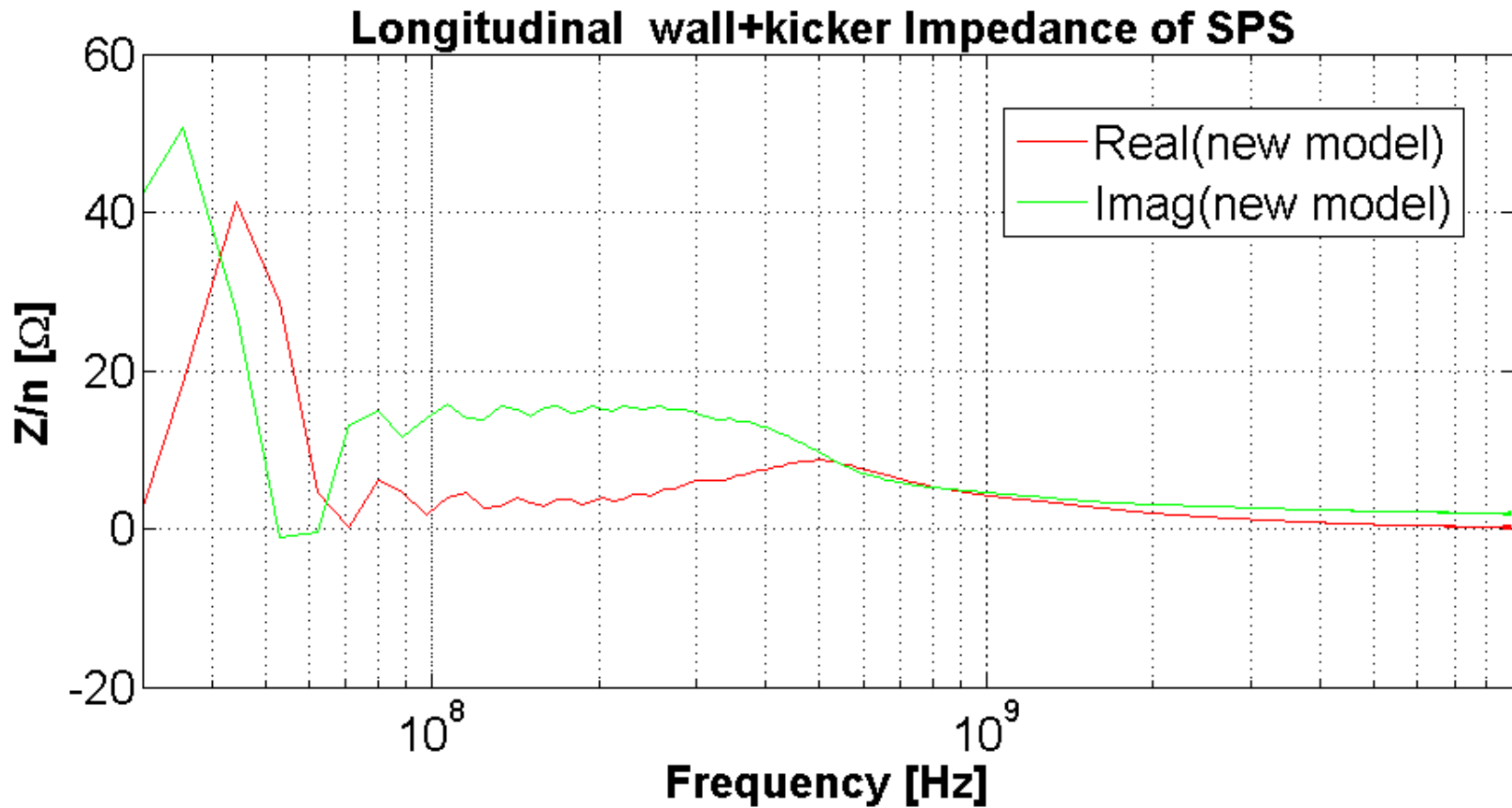
- The SPS kicker model was improved for a more accurate estimation of this relevant impedance contribution.
- The limitations of the coaxial wire method for impedance measurements are being investigated.
- Ferrite measurements were performed to validate the complex permeability model used in CST 3D EM simulations
- The SPS wall impedance model was improved accounting for the different vacuum chambers and the iron of the magnets

# Longitudinal SPS Impedance model



To be discussed with the RF team (possible sources, multi-bunch only single bunch etc.)

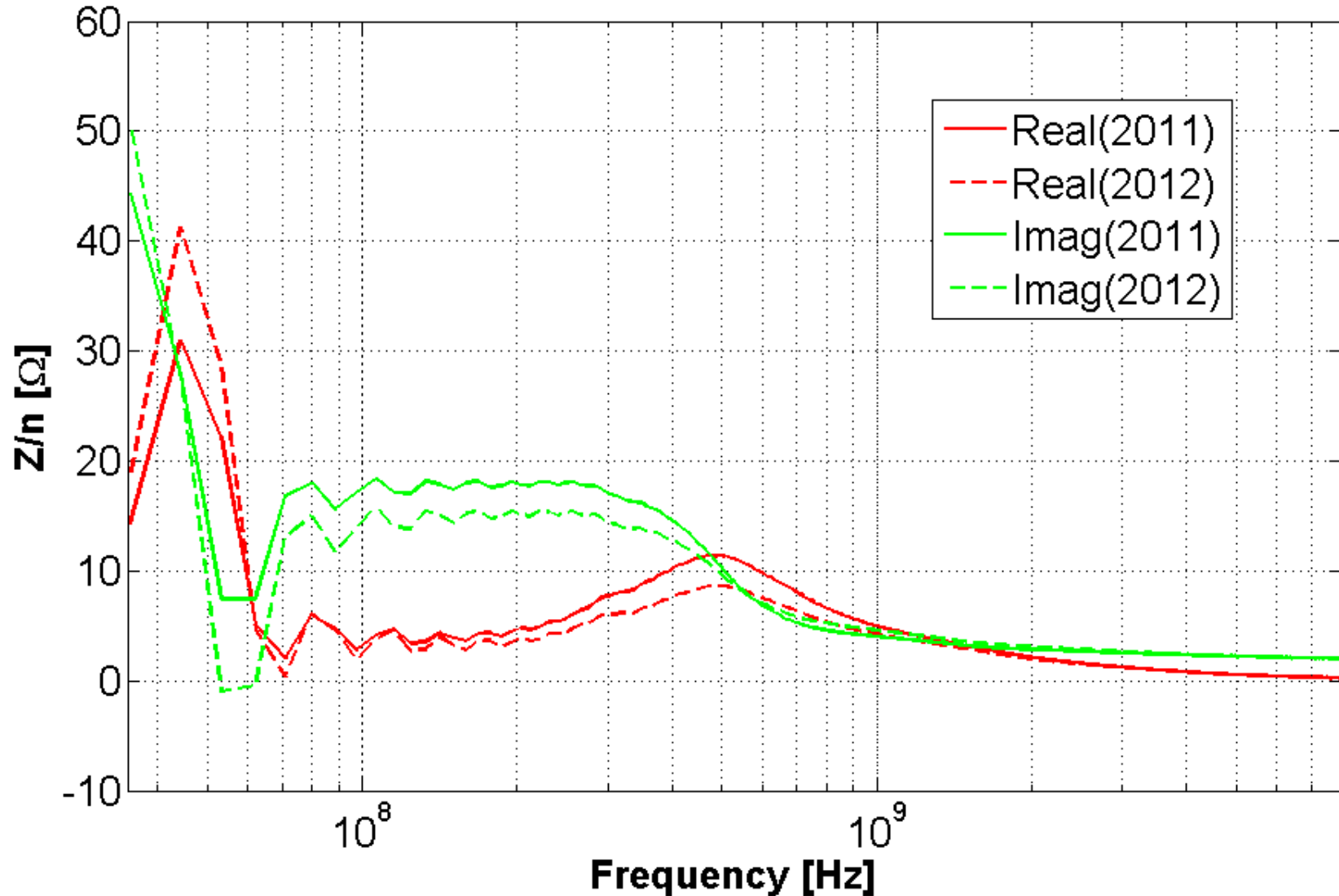
# Longitudinal SPS Impedance model



To be discussed with the RF team (possible sources, multi-bunch only single bunch etc.)

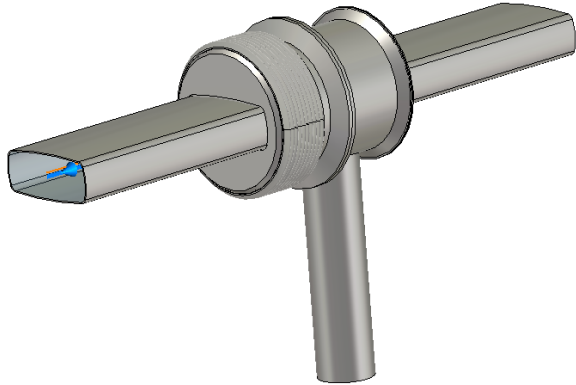
# Longitudinal SPS Impedance model

## Longitudinal wall+kicker Impedance of SPS

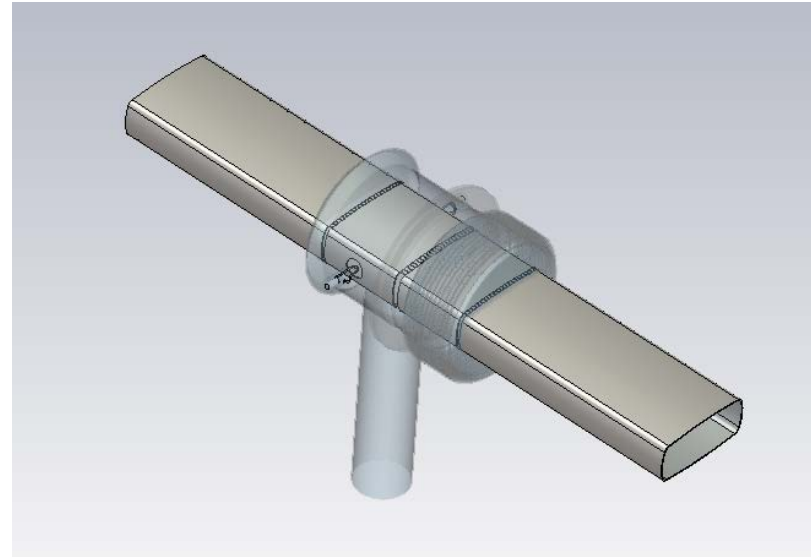


To be discussed with the RF team (possible sources, multi-bunch only single bunch etc.)

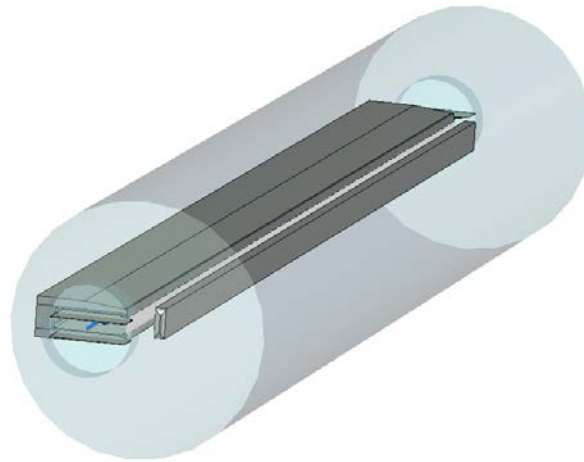
## Other devices that are not yet taken into account



SPS Pumping port

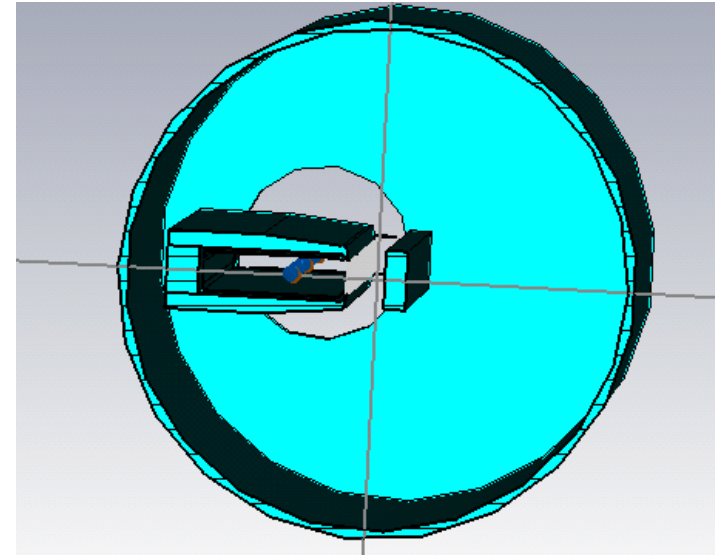
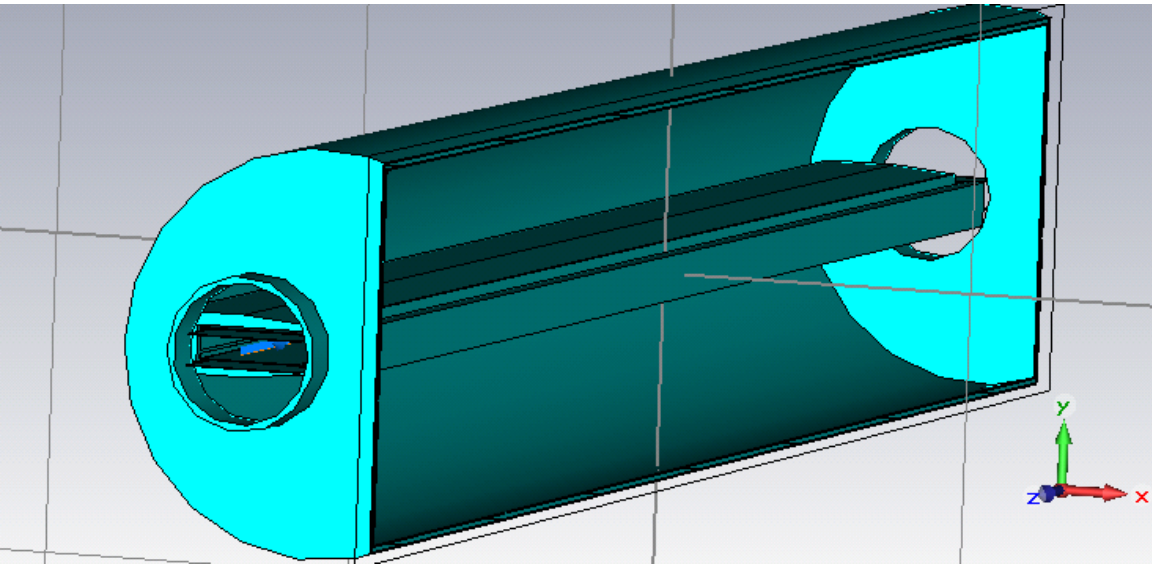


SPS Pumping port shielding and RF antenna



SPS electrostatic septum

# ZS simulations with CST (B. Salvant)

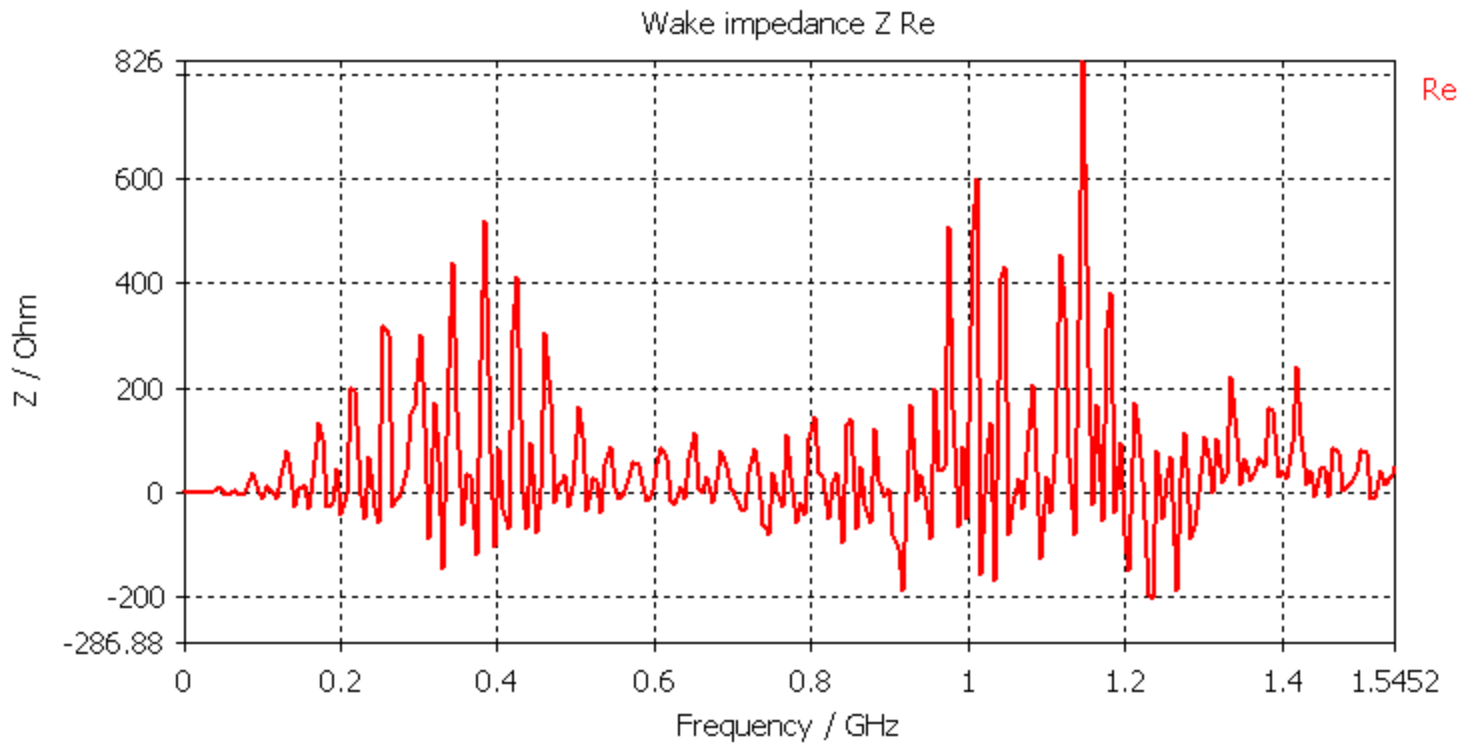


- Wires are tricky to simulate

Thanks to Bruno Balhan!

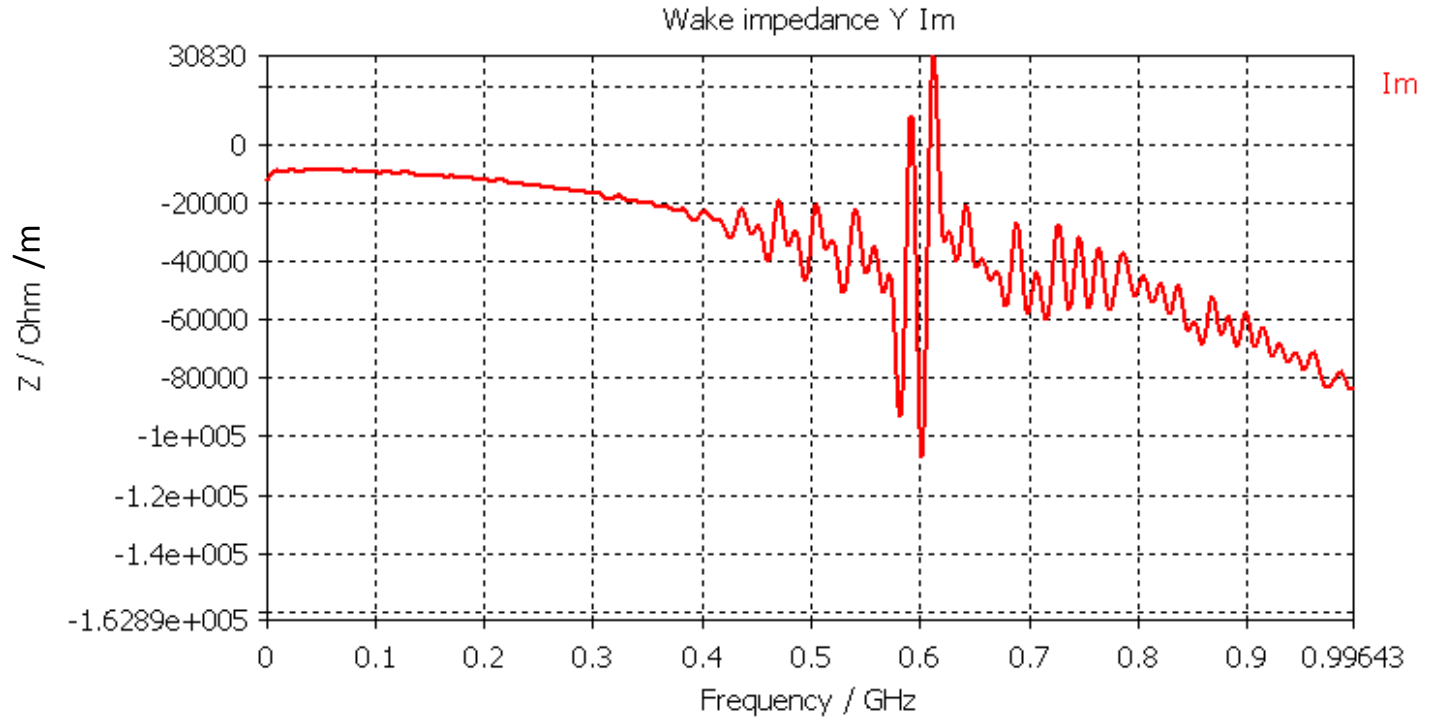


# Simulated longitudinal impedance



$\text{Im}(Z/n) \sim 0.02 \text{ Ohm}$

# Vertical impedance (imaginary)



$\text{Im}(Z_y) \sim 8 \text{ kOhm/m}$  (for 1 ZS)

# Measurements of Fritz presented by Elena at Chamonix 2001

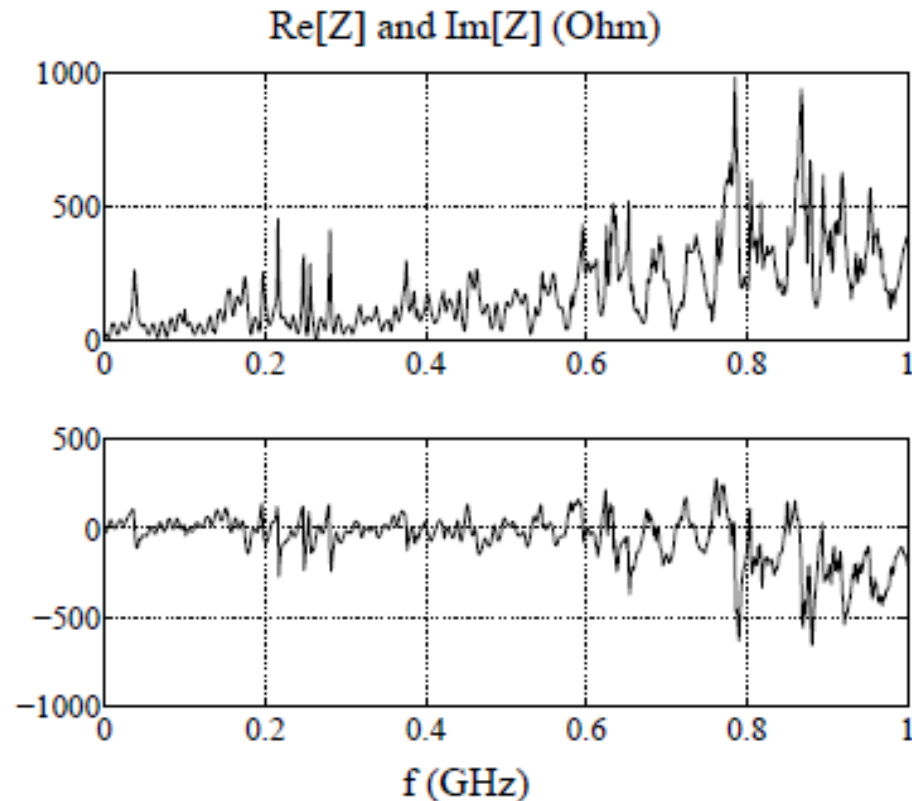
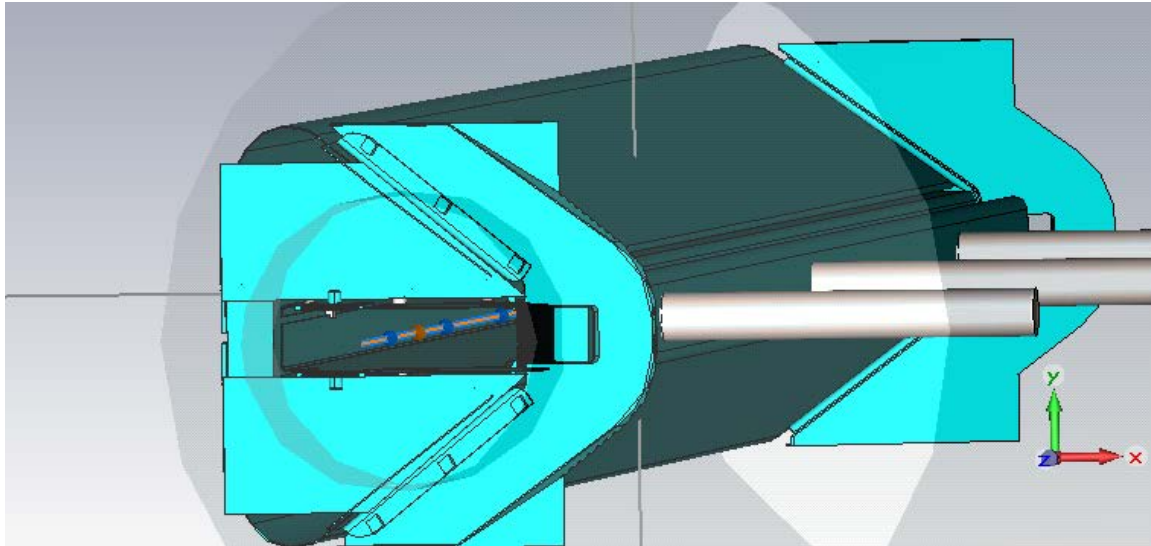
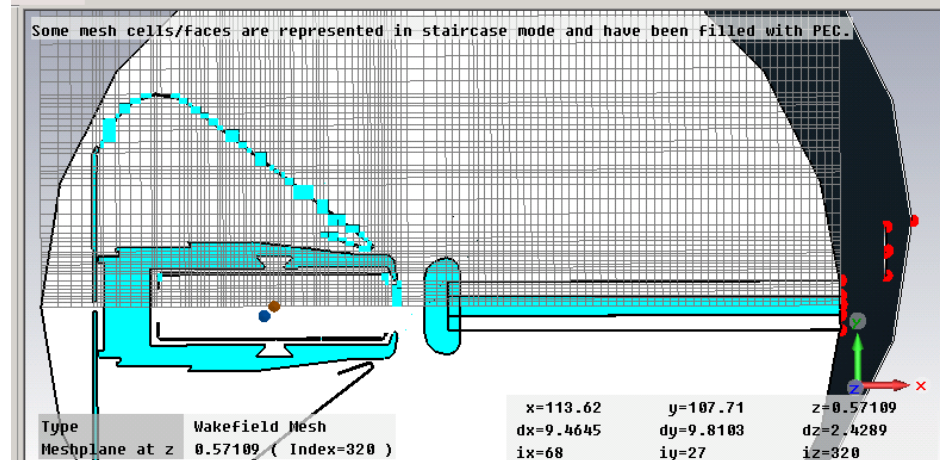


Figure 12: Real (top) and imaginary (bottom) parts of ZS impedance evaluated from the corrected values of amplitude and phase of  $S_{21}$  parameter.

# Imported structure from CATIA

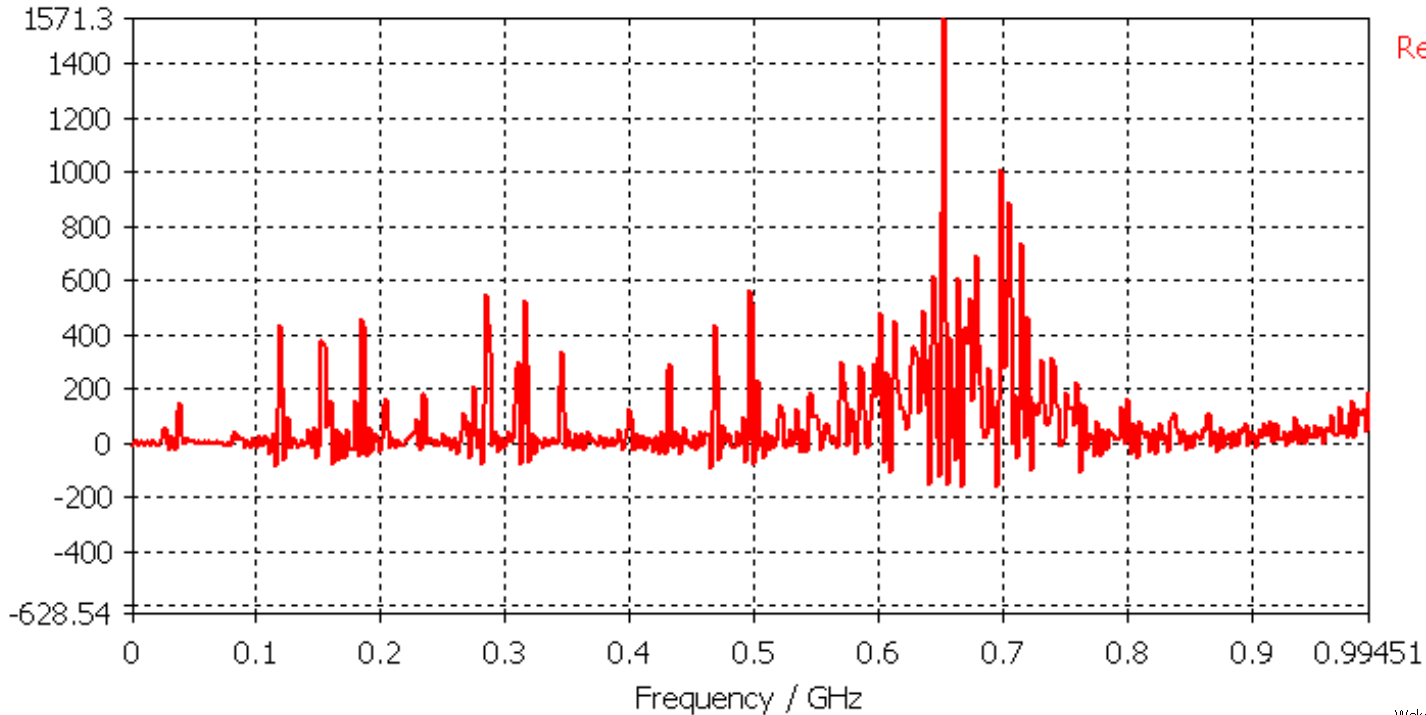


Very difficult to mesh properly,  
but we could assume the  
wires do not let the fields go through.



# Preliminary longitudinal impedance results with 60 m wake

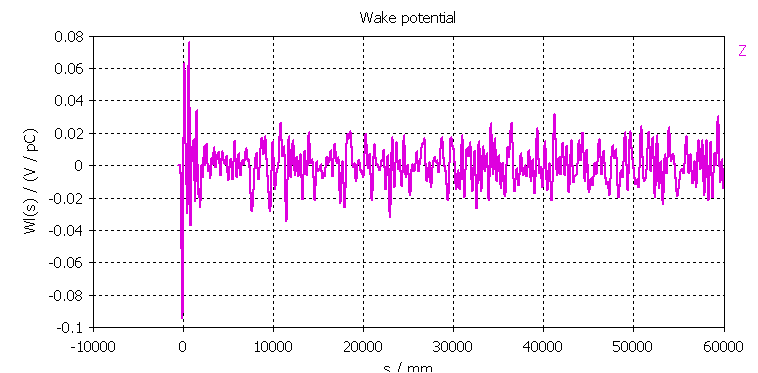
Wake impedance Z Re



Re

$\text{Im}(Z/n) \sim 0.04 \text{ Ohm}$

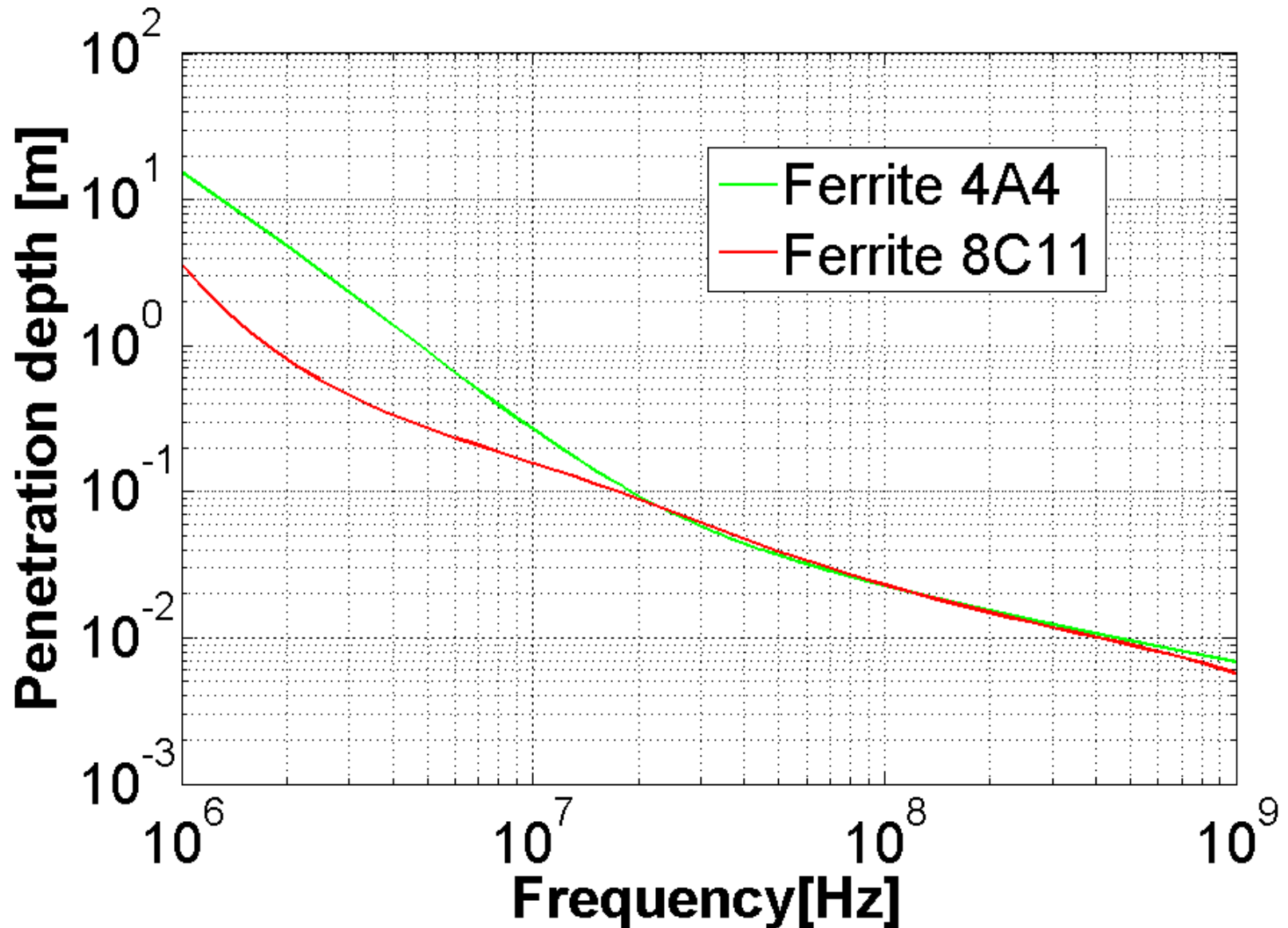
The height of the peak is underestimated →  
Are these peaks an issue?



Thank you for your attention

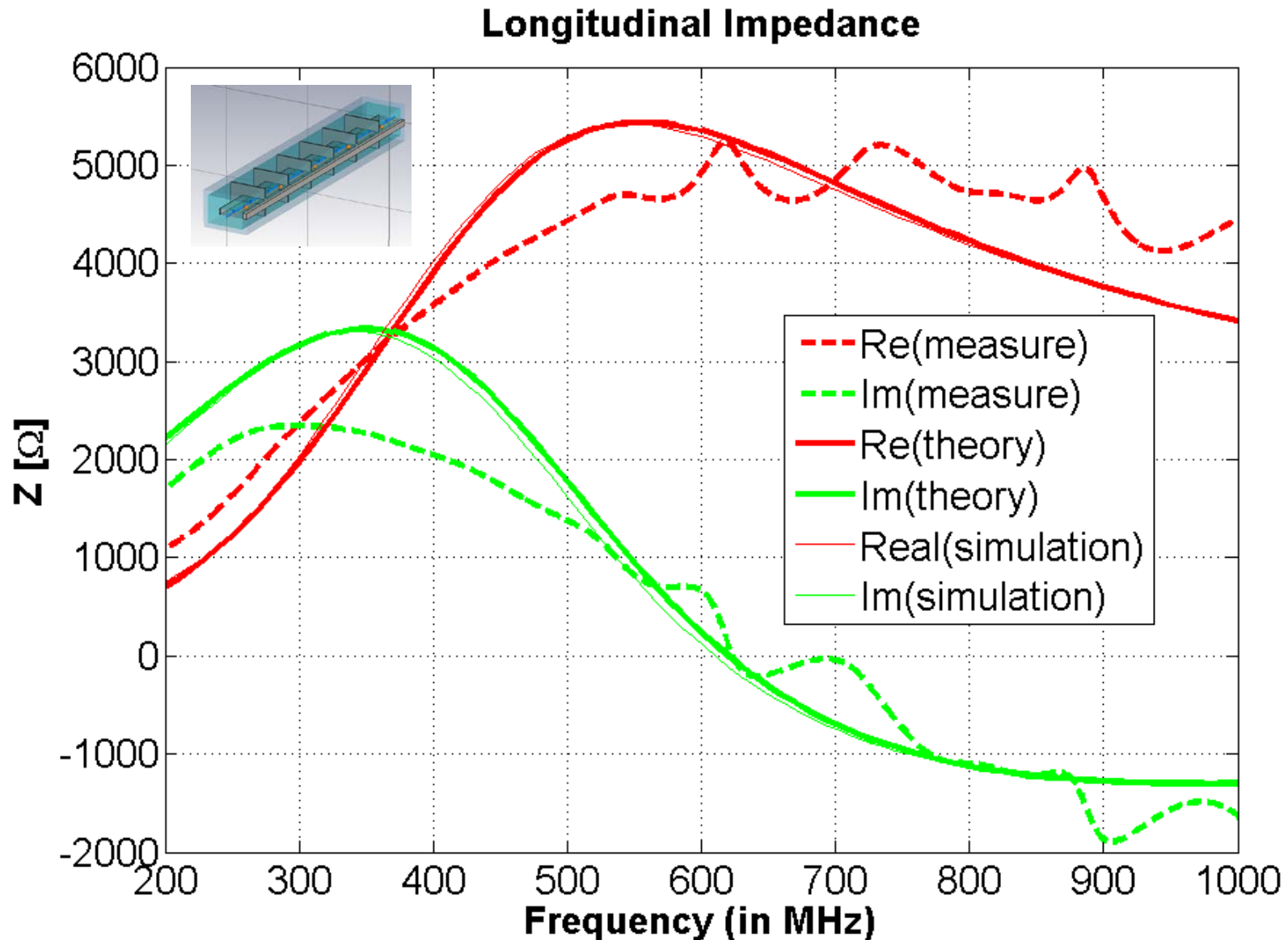
# Appendix

# Penetration depth in ferrite

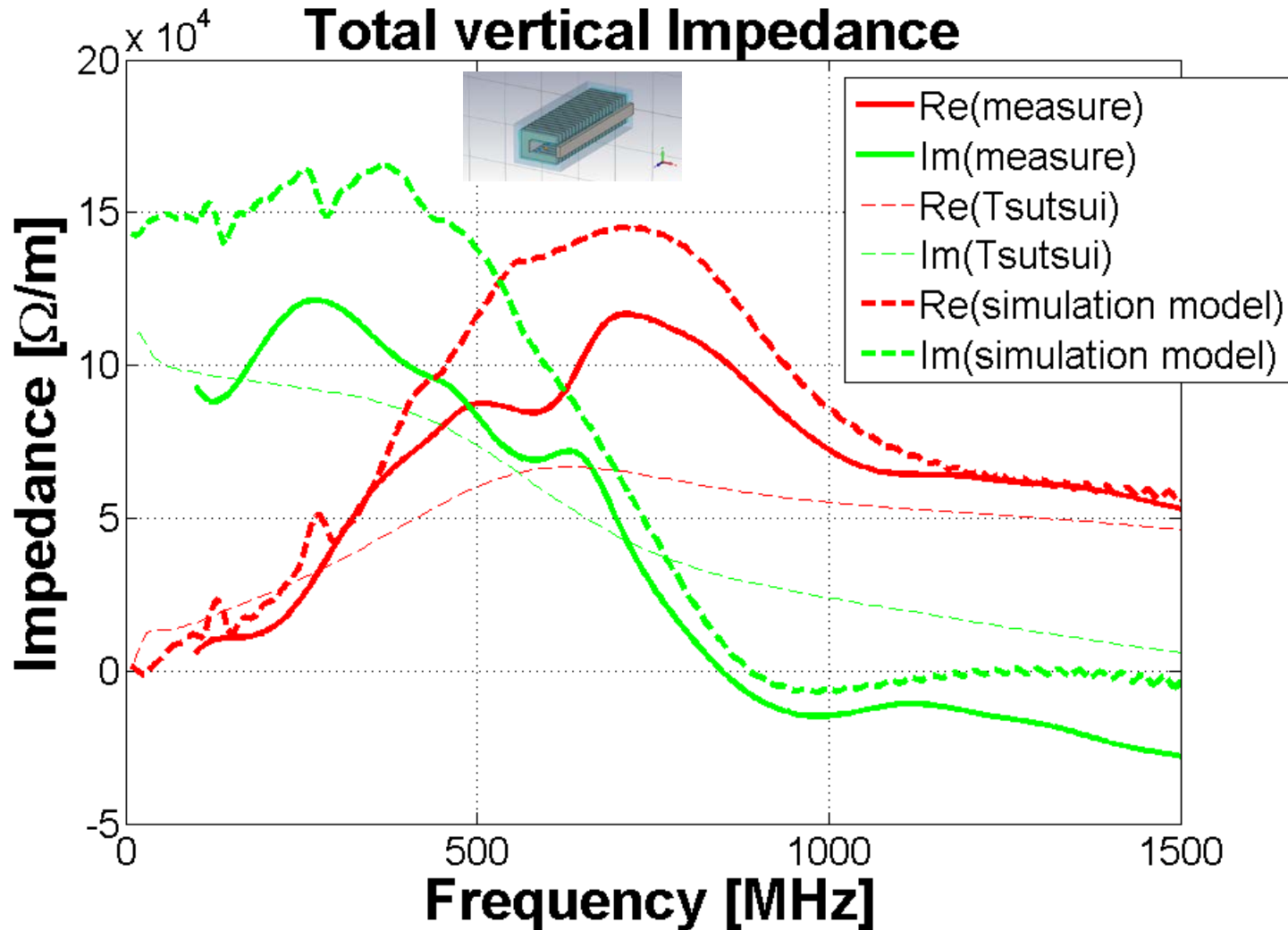




# Comparing longitudinal impedance: MKE-S

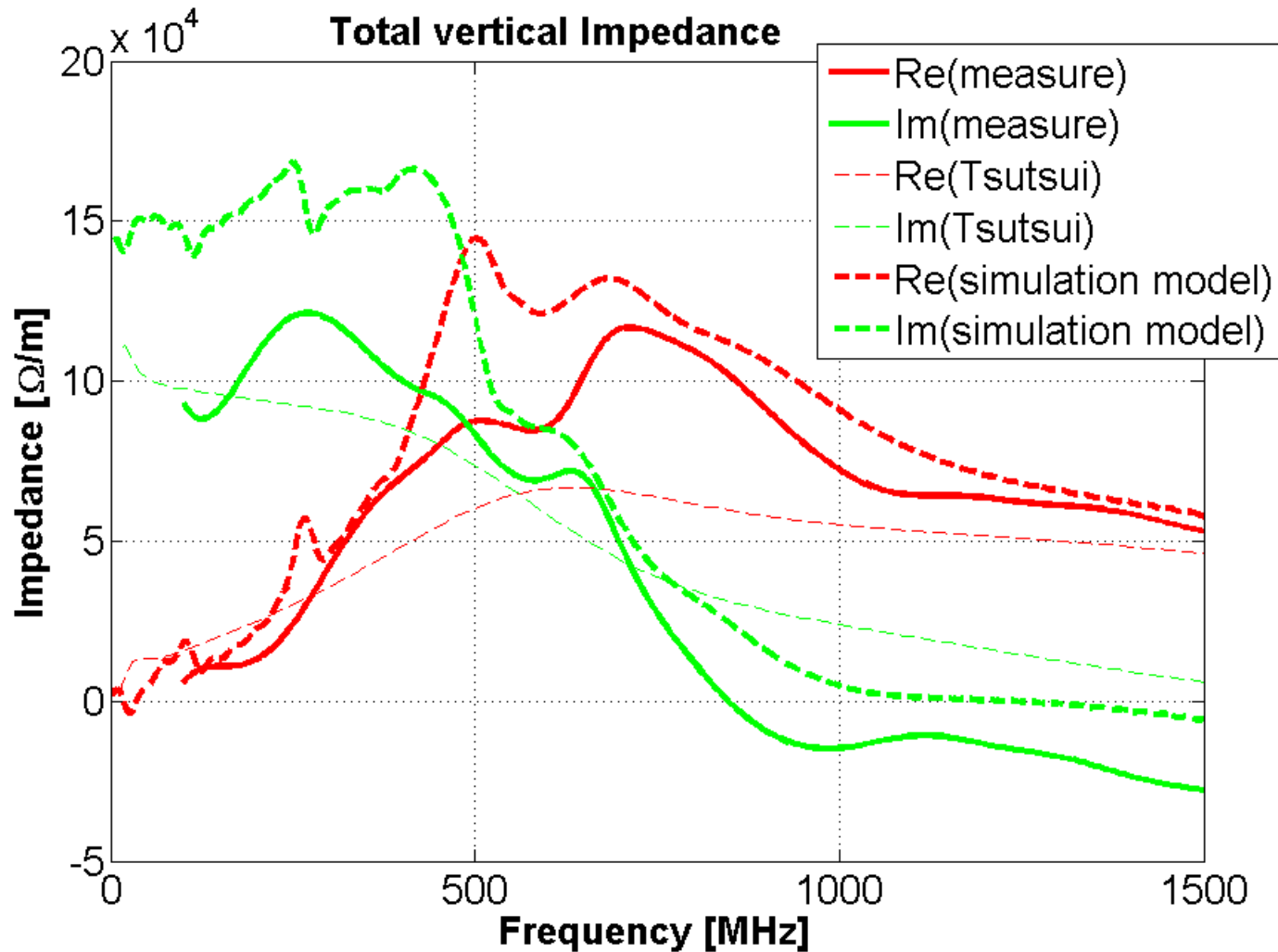


# Comparing total transverse impedance: MKP-L



Parasitic inductance of 100nH in parallel with the cell capacitance of 668 pF

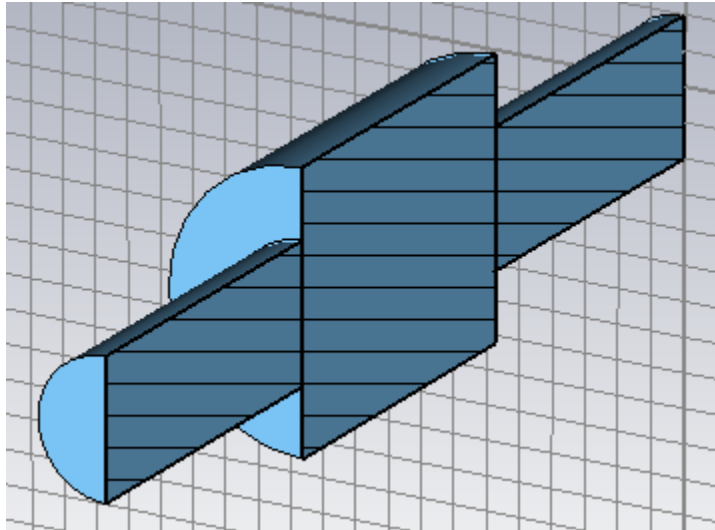
# Comparing total transverse impedance: MKP-L



Parasitic inductance of 100nH in series with the cell capacitance of 668pF

# Measurements of the coupling impedance using the coaxial wire method

The measured quantity is the transmission S21



cut-off frequency  $\neq 0$   
cut-off frequency = 0

TEM  $\rightarrow$  Propagation losses

Measured Losses = True Losses + Propagation losses

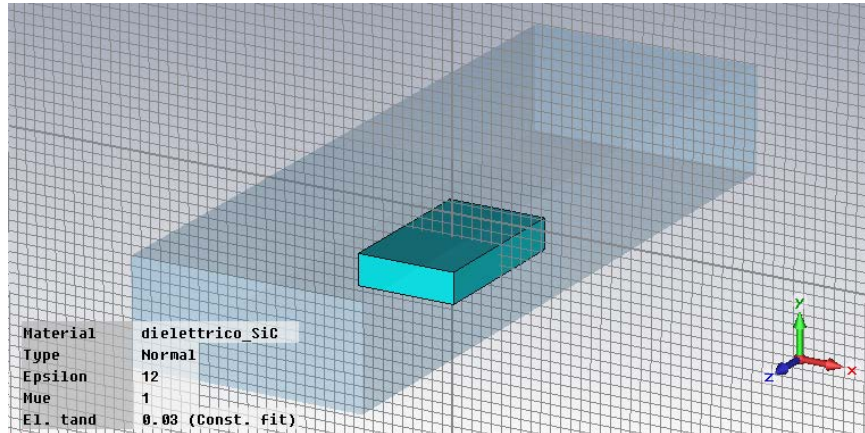
For resonant structures:

$$\frac{1}{Q_m} = \frac{1}{Q_{true}} + \frac{1}{Q_{prop}}$$

Due to the additional power transported by the wire the resonance should shift to lower frequency

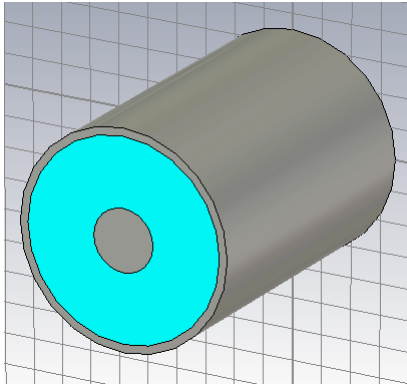
# Electromagnetic characterization of materials

We characterize the material at high frequency using the waveguide method



$$S_{21} = G(\epsilon', \epsilon'')$$

Coaxial line method



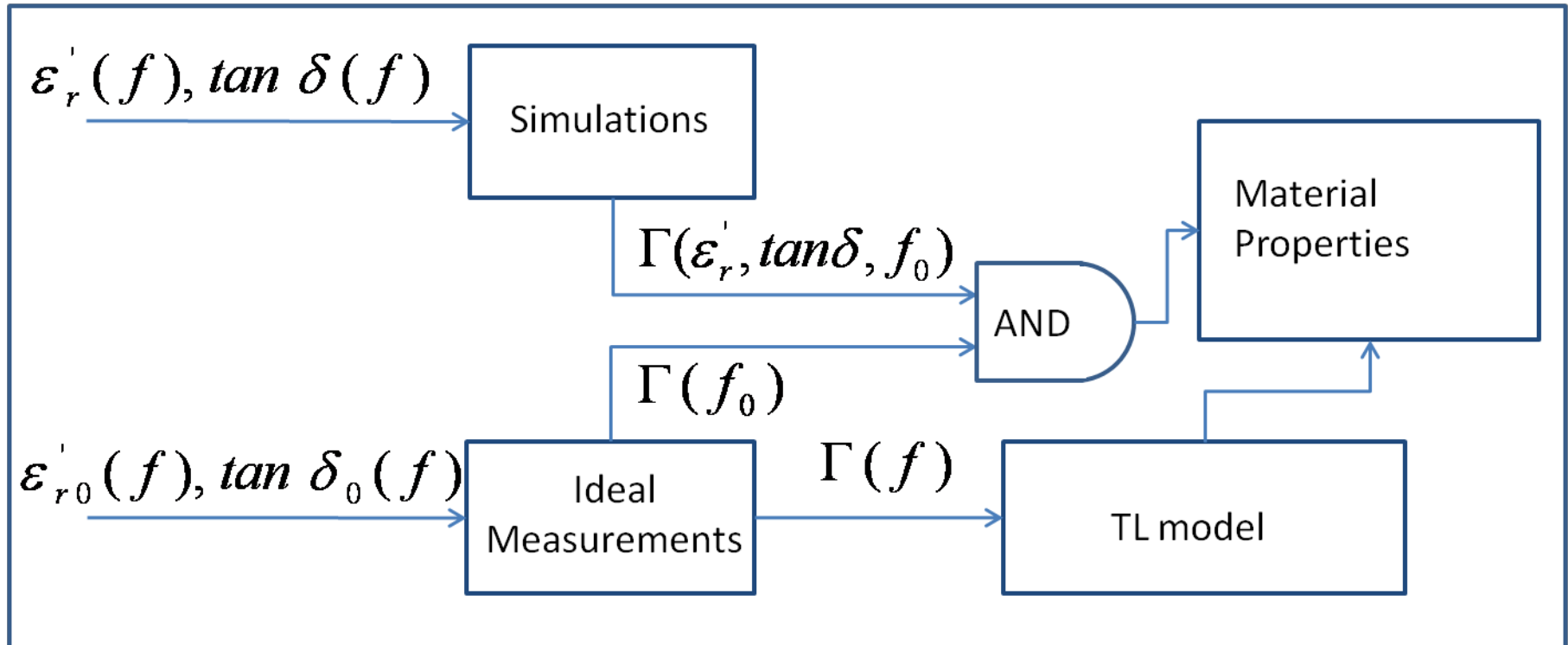
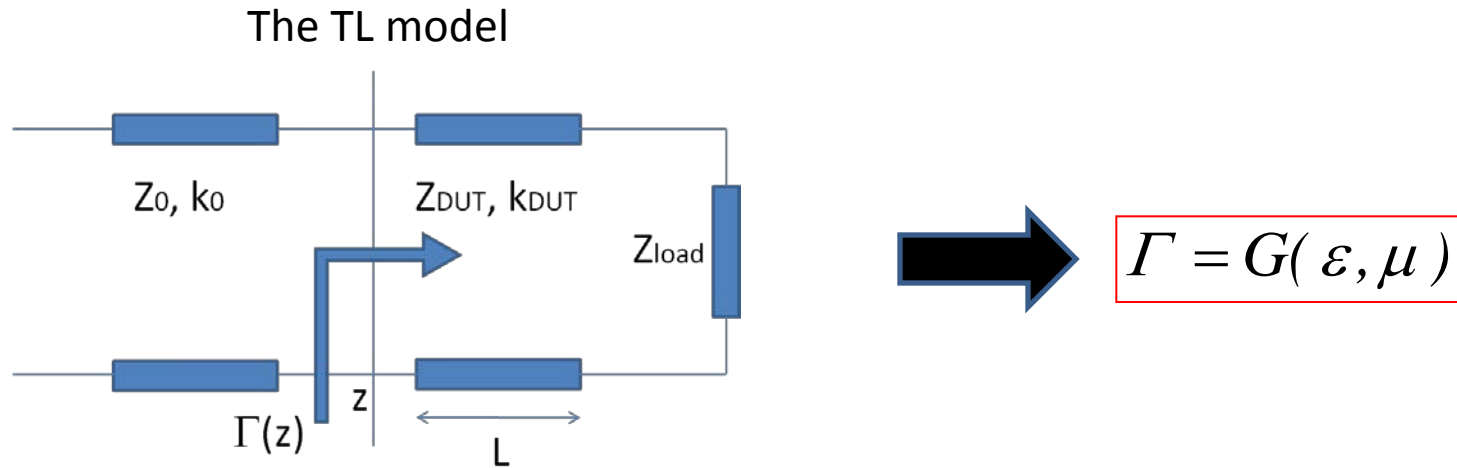
$$(\epsilon, \mu)$$

$$\Gamma = G(\epsilon, \mu)$$

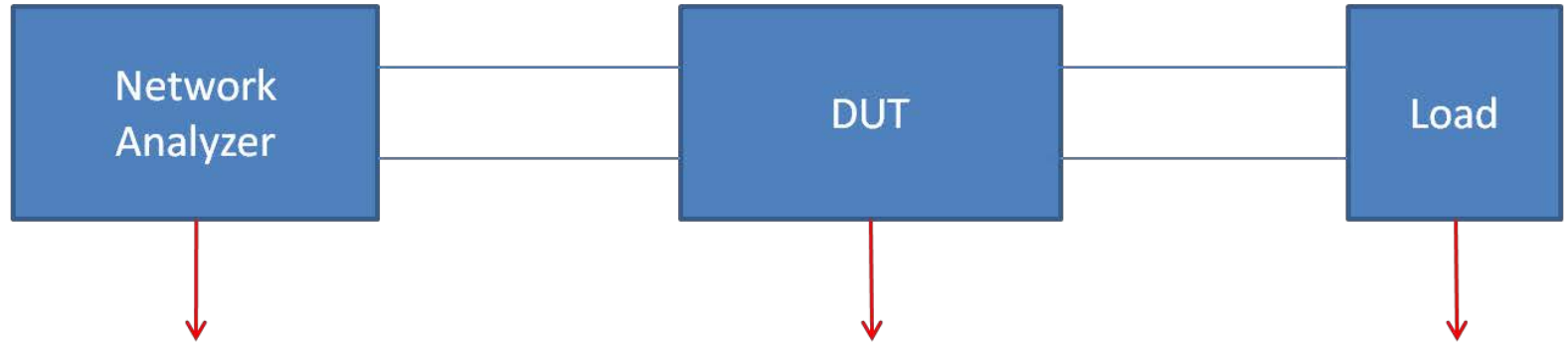


$$(\epsilon, \mu)$$

# The coaxial line method

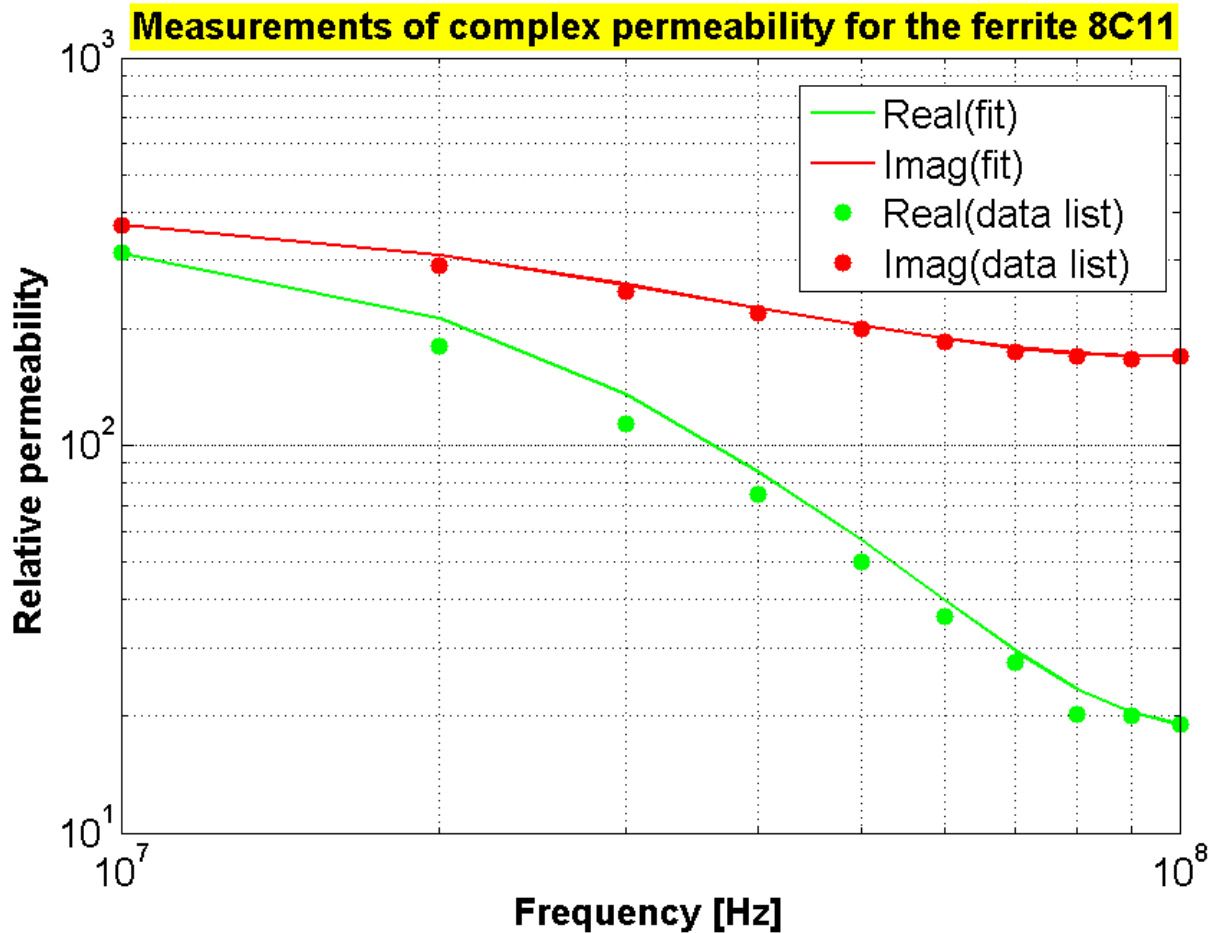


# Measurement setup



We did measurements for some SiC in the ranges 10 MHz-2GHz and 8 - 40 GHz and for the ferrite 8C11 in the range 10MHz-10GHz.

# Permeability measurements





# The effect of the iron (silicon steel)

## Iron (silicon steel) electromagnetic model

$$\mu = \mu_0 \cdot \mu_r = \mu_0 \left( 1 + \frac{\mu_i}{1 + jf2\pi\tau} \right) \quad \varepsilon = \varepsilon_0 \cdot \varepsilon_r = \varepsilon_0 \left( \varepsilon' - \frac{j\sigma}{2\pi f\varepsilon_0} \right)$$

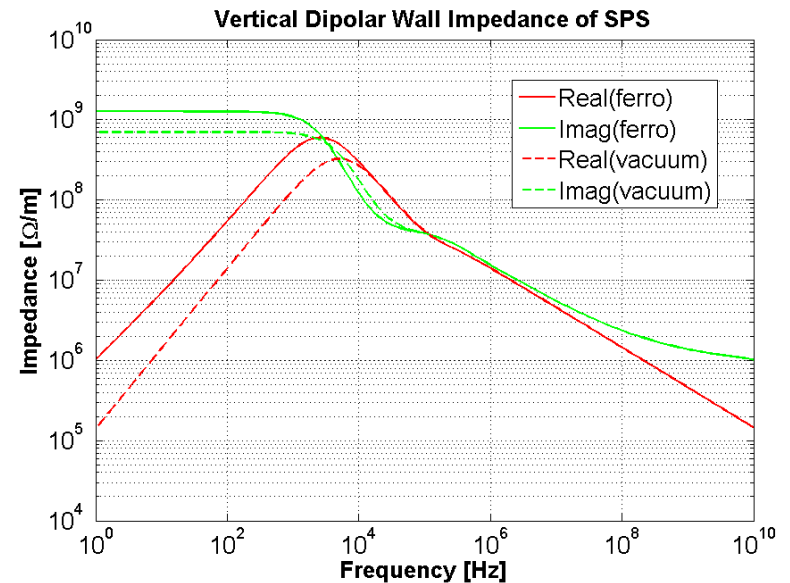
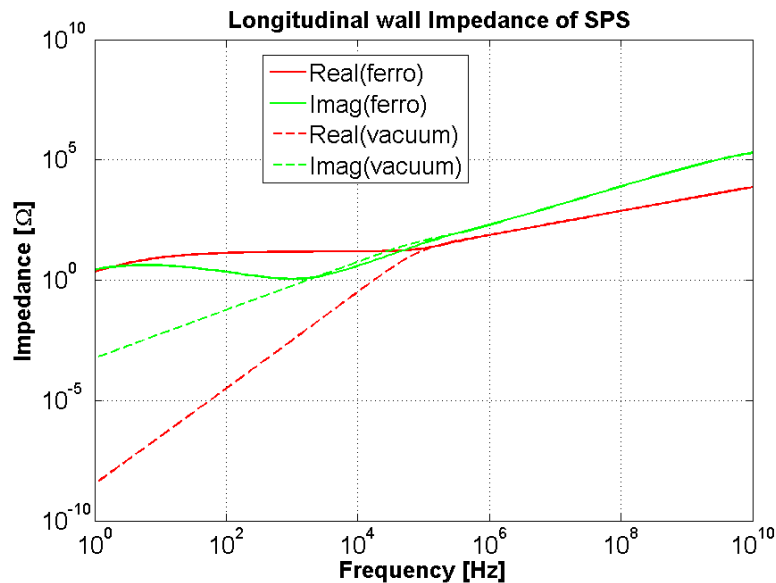
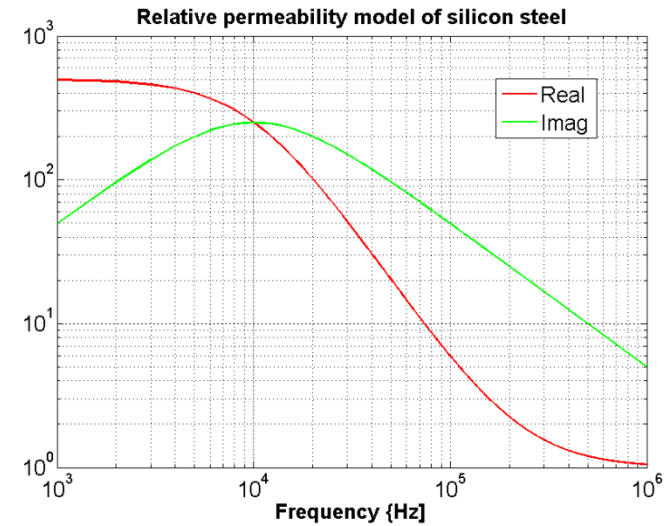
$$f_r = (2\pi\tau)^{-1} = 10\text{KHz}$$

$$\mu_i(\text{Injection}) = 500$$

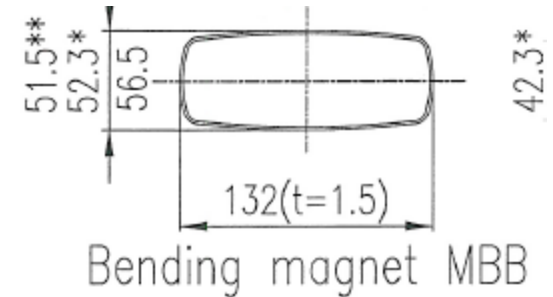
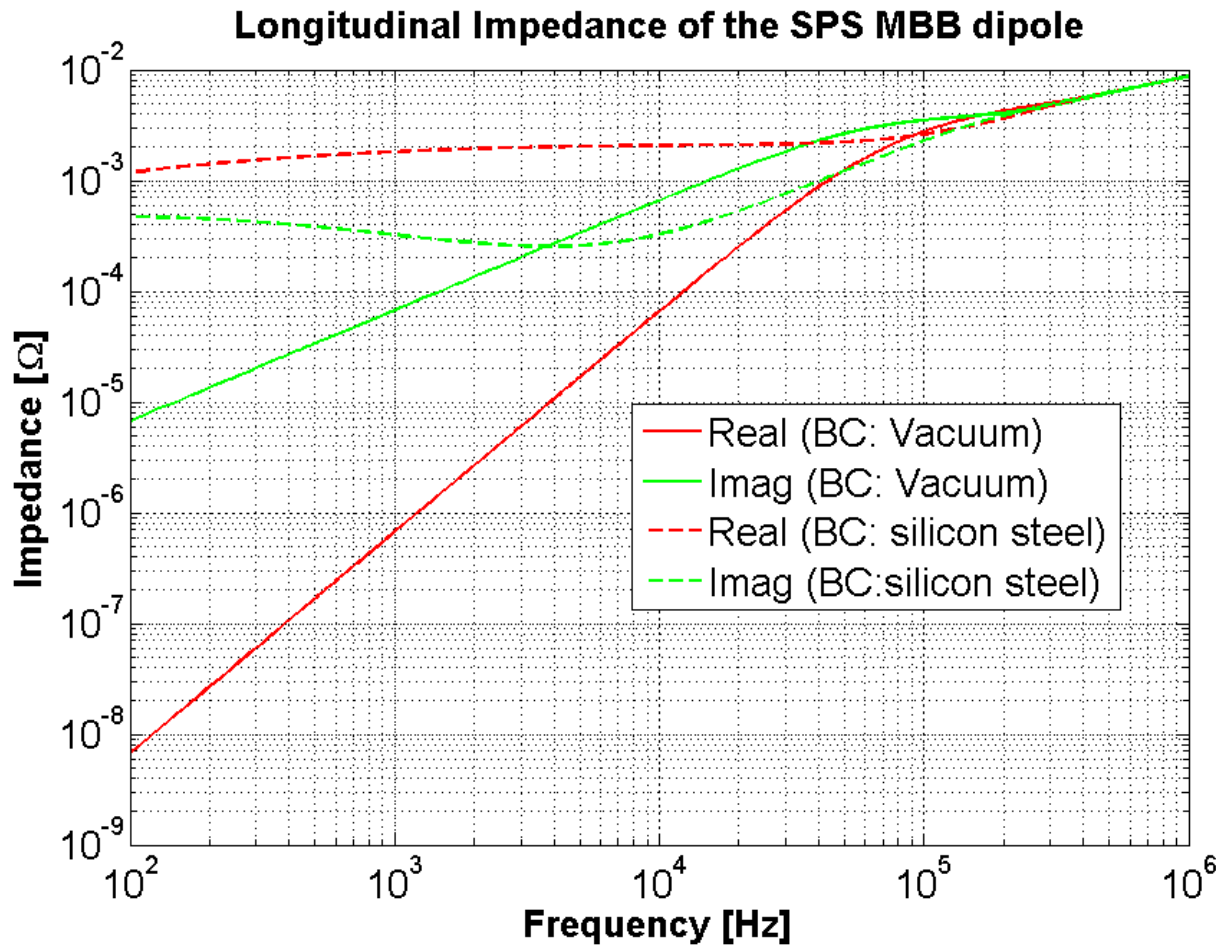
$$\mu_i(\text{Extraction}) = 33$$

$$\sigma = 10^5 [\Omega \cdot m]$$

$$\varepsilon' = 1$$



# Comparing SPS vacuum chamber with Vacuum and silicon-steel boundary



At low frequency the real part of the longitudinal impedance is much larger with silicon steel boundary